

cahiers d'informatique

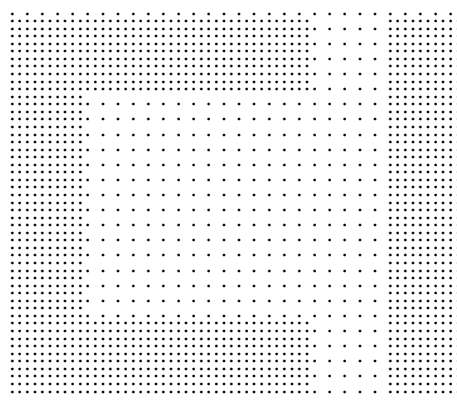
A RANDOM WALK ON AREA RESTRICTED  
SEARCH

SIMONE SANTINI

ESCUELA POLITÉCNICA SUPERIOR  
UNIVERSIDAD AUTÓNOMA DE MADRID

XXVI

cuadernosdeinformaticacomputingnotebooksquadernid'informatica  
arXiv:2006.14318v1 [cond-mat.stat-mech] 25 Jun 2020



The title of this series of technical reports constitute my homage to the legendary magazine *Cahiers du cinéma*, and to the role that it has played for many years in the creation of a widespread critical sense regarding film.

(C) Simone Santini, 2019

These notes constituted the class material for part of the syllabus of the graduate course "Caracterización de Redes y Topologías Biológicas" read during the academic years 2017-18 and 2018-19. I gratefully acknowledge the contribution of all the students of these classes who, with their interaction, have contributed to improve these notes.

Author contact: **[simone.santini@uam.es](mailto:simone.santini@uam.es)**



## 26.1 ARS, REWARD, AND DOPAMINE IN THE EVOLUTION OF LIFE

The starting point of these notes is a talk to which I heard few years back in Milan, Italy. The speaker, Giuseppe Boccignone, showed us the pair of images in Figure 26.1, which represent two paths in two dimensions. It is not hard to see that the macroscopic characteristics of these images are quite the same. Their most evident macroscopic feature is that they are heavily clustered: there are a bunch of points in a very restricted area and then suddenly the path jumps to a different area where a new cluster of points is created. The images are so

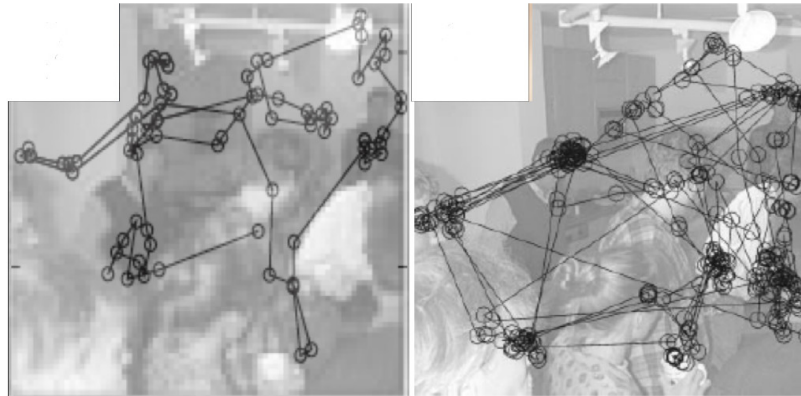


Figure 26.1: Two images that, apparently, describe the same phenomenon. While the paths displayed in the two images are qualitatively similar, their origin is quite different. The path on the right is a recording of the saccadic eye movements of a person looking at the image to which it is superimposed. The path of the left is that of a spider monkey (a monkey common in the Yucatan peninsula of Mexico) looking for food. The two paths are example of a common behavior found throughout the animal kingdom: *Area-Restricted Search*.

similar that one would have little trouble believing that they have been created by two instances of the same physical phenomenon. Yet, much to my amazement, Boccignone told us that this was not the case. The figure on the right shows the saccadic eye movements of a person looking at the picture that you can faintly see in the background; the picture on the left is the path followed by a spider monkey of the Yucatan peninsula while looking for food. It has nothing to do with the picture and was superimposed to it only to make the point more forcefully.

To find such a similarity in completely unrelated activities of two different species is as striking as it would be to find out that the ritualistic chant of a remote tribe in Papua has the same harmonic structure as the Goldberg Variations. Just as in the case of the tribe we would like to look for an explanation (maybe a previous contact with some Bach-loving explorer

that has been incorporated into the rituals of the tribe), so in this case it is not too far-fetched to start looking for some common underlying mechanism.

We are encouraged in our endeavor by the fact that the two behaviors do have indeed something in common: they are both examples of *search*. Search for visual information in one case, search for food in the other. So, we are on a hunt for a common mechanism that guides *search* in a wide variety of species under the most diverse circumstances. The mechanism must be very general, since it should apply not only to different species but also to very different levels of abstraction (from search for food in physical space to search for information in conceptual space).

The behavior that we observe in these two examples is commonly known as *ARS* (*Area Restricted Search*), a strategy that consists in "a concentration of searching effort around areas where rewards in the form of specific resources have been found in the past. When resources are encountered less frequently, behavior changes such that the search becomes less sensitive, but covers more space" [24].

As we shall see, the same basic mechanism permits *ARS* in a variety of cases and circumstances, from the foraging behavior of the nematode *C.elegans* to goal-directed cognition in people. You can have a personal experience of *ARS* by looking at Figure 26.2 and following the instructions in the caption (read the caption before looking at the pictures). *ARS* is incredibly widespread.

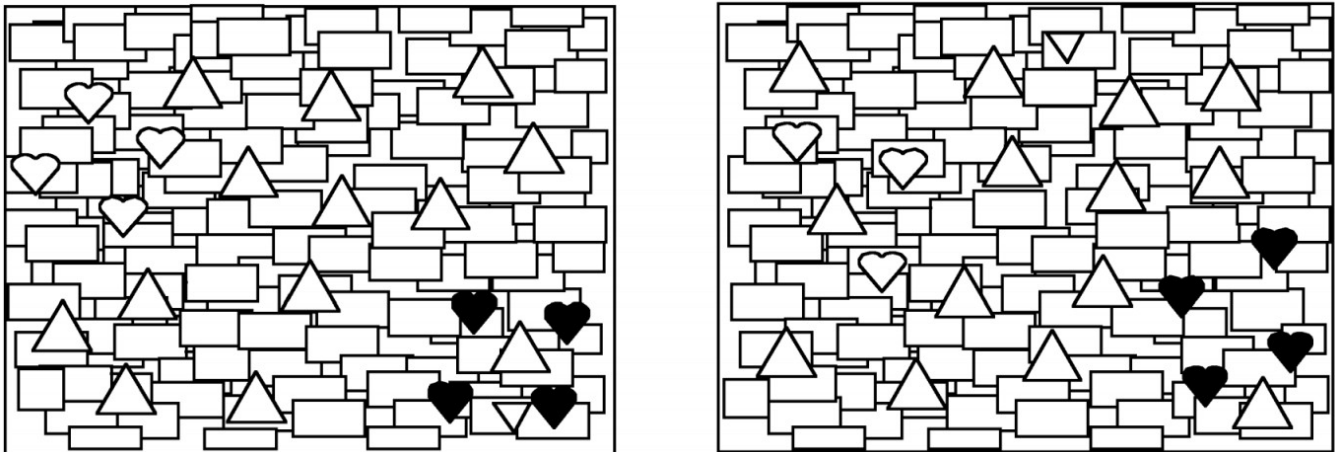


Figure 26.2: Paying attention to where your eyes look, begin in the left figure and look for the upside-down triangle (there is only one). Once you have found it, move to the figure to the right and look for the upside-down triangle there. Go ahead and do that now, before you read the rest of the caption. Where did you look first when you were looking for the triangle in the second figure? Did you look first near the black hearts? If you did, then you were performing *ARS*. You focused the attention in the area where you expected (based on your previous experience) the reward (the upside-down triangle) to be found and then, once you found out that your "confidence" area did not have the resource you were looking for, you started a rapid scan of the rest of the image, until you found the sought-after triangle.

Some form of it has been found in all major eumetazoan clades. To have an idea of what this entails, in Figure 26.3 I have drawn a very partial taxonomy of the animal kingdom. The clade on the left of the root, the *porifera* is composed of animals that do not have a real tissue: sponges and little else. The other clade, *eumetazoa* contains all other animals, from worms to mollusks to you and me. *ARS* can be observed, in some form or another, in the whole eumetazoa clade. This broad presence indicates that the mechanism behind *ARS* must have evolved quite

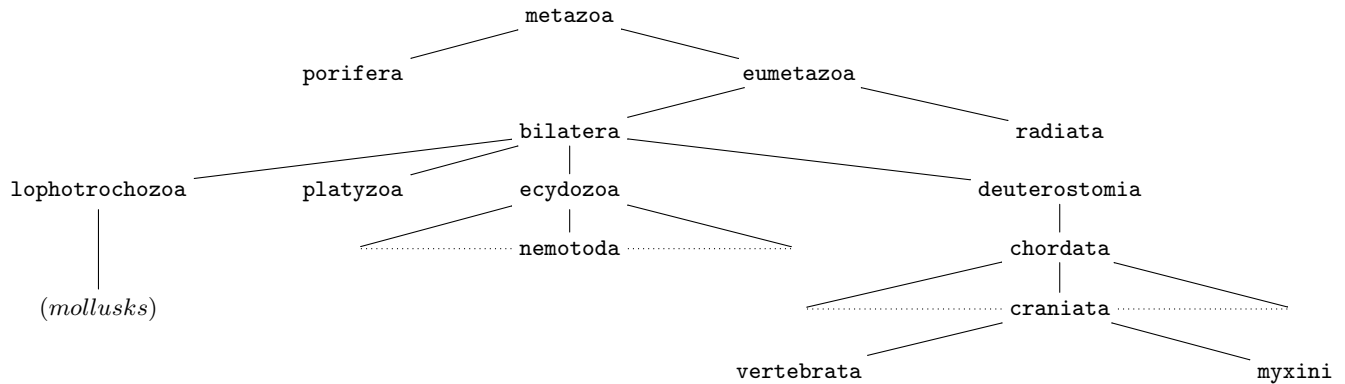


Figure 26.3: A (very small) fragment of the taxonomy of *metazoa* (i.e. animals). The group of *porifera* is composed of animals without tissue, and consists pretty much of sponges and little else. The clade of the *eumetazoa* contains all other animals, and in this whole clade ARS has been observed.

early, since the major divisions of the *eumetazoa* clade are very ancient, and it is reasonable to assume that all forms of ARS derive from a mechanism that was put in place before this division. ARS is, in other words, one of the basic mechanisms of life.

ARS might even be more basic than the *eumetazoa*: there are molecular mechanisms in protozoa that could be precursors of ARS. The most primitive example is the "run and tumble" movement of *E.coli* and *Salmonella typhimurium*. The movement of these bacteria is controlled by a flagellar motor. *Runs* consist of forward motion (longish stretch of resource search), while *tumbles* are made of random turns that keep the bacteria more or less in the same place (exploiting local resources while they last). Receptor proteins in the membrane bind these behaviors to external stimuli []. The mechanism on which ARS is based is, in its essential structure, fairly consistent across the whole spectrum of *eumetazoans*. Its fully formed presence in organisms with limited learning capabilities, such as *C.elegans* suggests that learning is not involved or, to the extent that it is (such as in mammals), it is based on a fully formed pre-learning machinery. This is what makes ARS so interesting: it is a basic mechanism that very different forms of life have adopted as a basic strategy to solve such diverse problems as looking for food in a Petri dish or trying to prove a mathematical theorem. Its omnipresence derives from the optimality of ARS as a search strategy in cases in which resources are "clumpy" and the information about the locations of the "clumps" is limited (we'll see that in the next section). In the case of foraging animals, the resource is food, and the reward is finding something to eat. In the case of somebody looking at an image, the resource is information about its content, and the reward is understanding what the image is about<sup>1</sup>. In all these cases, the animal or person moves locally around the same clump as long as it is rewarding to do so (viz. as long as locally one finds more food or new information), then starts moving rapidly to explore quickly new territory in search of a new clump.

The "reward" that one is after can be something very concrete (food) or something very abstract (the "Eureka" moment of proving a theorem) but in all cases the nervous system makes the reward

<sup>1</sup>Things are more complex in the case of looking at images: the actual paths that people's gaze follow depend on what they are looking for. Given an image of an interior, the actual paths are different if the subjects are asked e.g. "From what epoch is the interior?" or if they are asked e.g. "What are the people in the image doing?" This is not important for our present considerations: all these paths, different as they may be, exhibit the features of ARS.

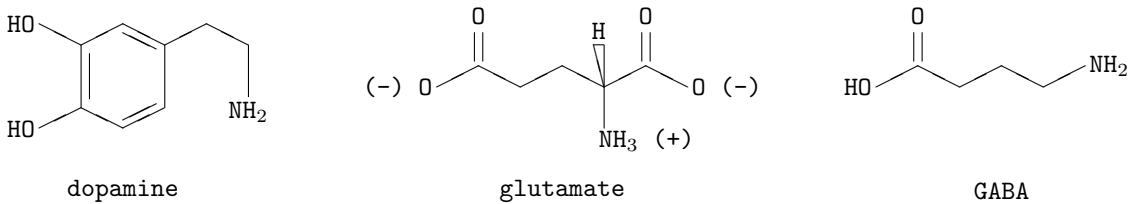


Figure 26.4: Three neurotransmitters that will figure in our discussion. Simplifying things very (very!) much, glutamate has essentially an excitatory action: its release in a synapse will move the postsynaptic neuron closer to firing. GABA is, on the contrary, inhibitory, its release will make the postsynaptic neuron less likely to fire. Dopamine is a modulator of glutamate.

substantial by encoding it as the release of a very specific chemical: *dopamine* (figure 26.4). The organism in which the molecular basis of ARS is best understood is the nematode *C.elegans* [23]. The neural circuitry consists of eight sensory neurons presynaptic to eight interneurons that coordinate forward and backward movements. The sensory neurons alter the turning frequency by releasing dopamine on the interneurons, modulating the reception of glutamate (Figure 26.5). External administration of dopamine increases the turning frequency, while administration of a

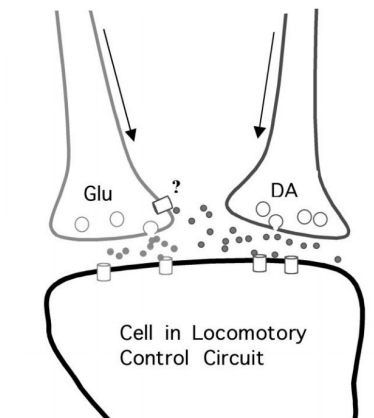


Figure 26.5: Dopaminergic action in *C.elegans*. Glu and Da represent glutamatergic and dopaminergic presynaptic neurons, respectively. The release of dopamine from the dopaminergic neurons alters the postsynaptic neuron's response to glutamate. It is not known whether this is due to a presynaptic response of the glutamatergic neuron and/or to a postsynaptic response of the locomotory neurons (from [23]).

dopamine antagonist reduces it [23]. A reasonable model of *C.elegans* behavior suggests that, while on food, the sensory neurons release dopamine, which, via the action of the glutamate, leads to increased switching behavior in the interneurons, resulting in more turns and, consequently, in a trajectory that stays local. When off food, the dopaminergic activity is reduced, and the interneurons reduce their switching frequency, leading to less turns and more ground covered

Although *C.elegans* is the only organism for which the neuromolecular mechanism of ARS is well understood, there is strong evidence of dopaminergic modulation of glutamatergic synapses throughout the major clades of the eumetazoans [1, 9]. In insects, for example, dopaminergic neurons in the abdominal ganglion are sparsely distributed, but show large branching patterns,



1. lateral medial
2. globus pallidus
3. striatum

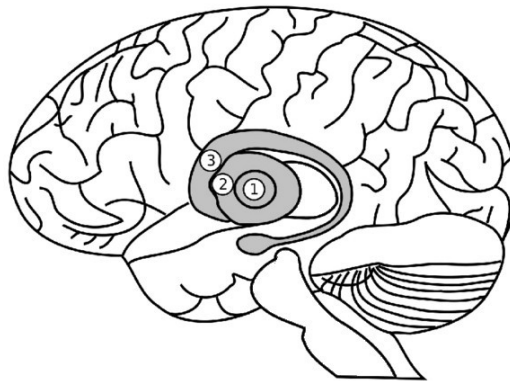


Figure 26.6: The basal Ganglia and, specifically the striatum have a large number of dopaminergic inputs from other parts of the brain, and are involved in ARS. While in simple animals like *C.Elegans* ARS is in a simple pathway from sensory input to motor neuron, in mammals the input comes from other areas of the brain, and the output acts on the cortex, making it possible to use ARS for more abstract problems than the immediate search for food.

indicative of neuromodulation [30].

The relation between dopamine and ARS has been documented throughout the invertebrates, especially in the fruit fly *Drosophila melanogaster* [2], in crustaceans [20], in *Aplysia* [12], etc. In all these cases, ARS is limited to food search which is, clearly, the search problem for which ARS first evolved.

In vertebrates, the modification of behavior by dopamine increases in complexity and begins to involve behavior not directly related to food. For example, in frogs and toads dopamine modulation is involved in the visuomotor focus on preys [7]; similar dopaminergic involvement in visuomotor coordination can be found in rats and humans [3, 13, 16]. This finding is significant in that it indicates a strong relation between ARS and *inhibition of return*: the fact that viewers show significant latency in revisiting objects or regions of a scene that have already been investigated, united to the lingering of saccadic movements in regions of interest [43].

The important change in vertebrates is the extension of ARS-like behavior to cover not only actions with an immediate reward, such as the search for food, but also situations in which the reward is projected or even in which the reward itself is a neural state. The detachment from the immediate food rewards is what makes it possible to adapt ARS to abstract functions such as *goal-directed cognition*. It seems, in other words, that when new problems arose that had the same abstract structure as search for food, animals, rather than developing a new mechanism, coöpted the dopaminergic modulation that guided food search to work on the new problem.

The most important neural structure associated with goal-directed cognition is the *basal ganglia* and, more specifically, the *striatum* [11, 35] (Figure 26.6). Information enters the basal ganglia through the striatum, and a great number of the inputs to the system are dopaminergic [36]. The structure of the basal ganglia and much of their connectivity are maintained across vertebrates [37]. The major change from anamniotes (fish and amphibians) to amniotes is the

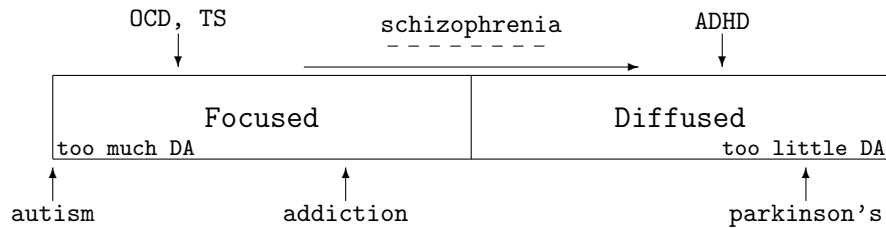


Figure 26.7: The continuous arrow at the top represents the normal temporal progression of dopaminergic activity in ARS, modulating behavior from focused (i.e. local) search to diffuse (i.e. global). The placement of the pathologies is qualitative and not based on a model but on the fact that they are treated either with dopamine or with dopamine antagonists. Although dopamine seems to be a factor in these diseases, there are clearly more factors at play. Schizophrenia is the most emblematic case in which the mechanism is not well understood, as reflected by its ambiguous positioning via the dashed line. OCD is *Obsessive-Compulsive Disorder*, TS *Tourette Syndrome*, ADHD *Attention Deficit Hyperactivity Disorder* (from [24]).

proliferation of dopaminergic neurons that input to the striatum [36], while the structure of the striatum stays pretty much the same.

The balance between glutamate and dopamine in the striatum is key to the proper functioning of ARS-like activities, and an imbalance between the two neurotransmitters is suspected in a number of pathologies affecting goal-directed cognition, including Parkinson's, schizophrenia, and addiction. Many of these conditions can be regarded as radicalization of ARS in one direction or another (too local or too global) due to imperfect dopamine control (see Figure 26.7). In the striatum, dopaminergic neurons modulate the glutamatergic input at the tips of spiny neurons. The action of the dopaminergic inputs appears to perform a neuromodulation of the strength of the glutamatergic inputs (Figure 26.8) The mechanism is similar to that described for *C.elegans* in Figure 26.5, but in the mammalian striatum the shape of the spiny neuron has specialized for this function and the inputs, several magnitudes higher in number, come primarily from connections to cortical neurons rather than directly from sensory neurons as in *C.Elegans* [45]. However, at the level of the microcircuit, little has changed from nematodes to amniote vertebrates. The origin of the dopaminergic input does, however, mark a fundamental evolutionary shift in the activity range of ARS-like behavior. While in *C.elegans* or *Drosophila* the afferent dopaminergic signal is reliably related to the presence or absence of food, in higher vertebrates the signal may represent the expectation of a reward. The critical transition here is from a concrete (directly sensed) reward to its neural representation that is, from a physical reward to the abstract idea of a reward [39]. As Hills puts it: "the evolutionary theory [of ARS] is therefore completely consistent with the reward theory of dopamine, but adds the evolutionary hypothesis that the initial reward represented by the release of dopamine were food. Only later was this system co-opted to represent the expectation of a reward, which allows for goal-directed cognition" [24].

To conclude this brief excursus of ARS, we consider a region of relatively recent evolution that, outside of the basal ganglia, is heavily involved in goal-directed behavior: the *prefrontal cortex* (PFC). The PFC has clearly evolved much later than ARS; nevertheless, it is

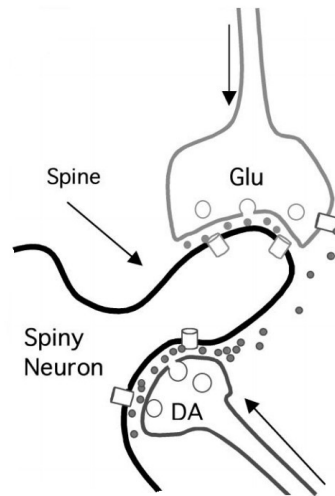


Figure 26.8: The dopaminergic-glutamatergic interaction in the synapses of spiny neurons in the mammalian striatum. Glu and DA represent glutamatergic and dopaminergic pre-synaptic neurons, respectively (from [24], redrawn from [10]).

heavily involved in goal-directed behavior via massive connections to the striatum [31]. Dopamine has been shown to be a factor in the sustained activation of the PFC [40, 44]. Most models of PFC see the rôle of dopamine as holding objects in attention long enough for appropriate behavior to be activated [6]. Consistently with ARS, already known solutions mediated by the PFC are most typically tried when a problem has to be solved in a new situation [14].

The context in which goal-directed cognition takes place includes external and internal stimuli; ARS depends in part on the alignment of external stimuli with previous expectations. This is likely to be controlled by the connections between the PFC and the *Nucleus Accumbens* (NAcc) in the striatum, which modulates attention, eye movements, and the maintenance of working memory [5, 17, 38]; dopamine has been identified as one of the main influences in the modulation of NAcc activity [18]: novel stimuli lead to increase in dopamine in the NAcc and in the PFC [4].

So, in the evolution of vertebrates, we see a progressive extension of the rôle of ARS, from the dopaminergic control of visuomotor control in frogs and toads to the similarity mediated maintenance of ideas in working memory [39]. ARS appears therefore to be one of the fundamental strategies in the animal kingdom, co-opted and adapted to a number of situations, from the "run and tumble" behavior of *E.coli* to the way we focus on and later abandon ideas when we think about a problem.

\* \* \*

This brief explanation of the evolutionary basis of ARS has been centered on its molecular mechanism, especially on the rôle of dopamine as neuromodulator. From now on, however, our focus will change: we shall try to understand the exterior characteristics of the behavior. ARS leads to a well identified patterns of motion either in the physical space (in the case of foraging), in the visual space (scanning an image), or in any number of abstract spaces. We

shall study mathematically these patterns of motion and try to characterize them. Our methods will be based mostly on the study of random walks, of diffusion, and on the kinds of anomalous diffusion to which ARS leads.

## 26.2 OPTIMALITY OF ARS

The evolutionary success of ARS entails, according to the theory of natural selection, that ARS is an optimal strategy---if not globally, at least locally---for a large set of problems. In abstract terms, we have a space with certain resources placed in different parts of it; we need a strategy to navigate this space collecting the greatest amount of resources. This must be done without information on the placement of the resources. (If we can sense from afar where the resources are located, we simply walk there and get them: no search strategy is necessary.) The nature of the resources can be the most diverse: in the case of foraging (to which we shall mostly make reference), the resource is food; in the case of saccadic movements, it is the visual information that we get from the visual field, and so on. ARS is optimal if the resources are "patchy," that is, if they are organized in resource-rich patches separated by areas of small or zero resource concentration. In the model that we shall develop in this section, we assume that the resources are consumed in the course of the activity, and that they are not replenished while the activity goes on. Resources are consumed simply by moving on top of them (assuming that, after walking on them, they would be consumed with a certain probability would not substantially change the model). In the example of food, this means that we have food distributed in patches (a grove, a pond, a herd, a school of fish...) and the forager moves inside the patch and between patches eating what it finds. We make a number of hypotheses. Firstly, we assume that the food doesn't move around or if it does (as is the case of animal preys) its movement is not significant and food can be modeled as static. Secondly, we assume that the forager will eat all the food it can find as soon as it finds it (its eyesight is perfect and its appetite endless). Finally, food doesn't grow back: once it has been eaten at a particular location, that location will remain barren for the rest of the forager's activity. In the case of saccades, we assume (as is often the case) that there are patchy areas in the visual field that are rich in information useful to interpret the scene (relevant or telling objects, faces, etc.). We also assume that once we have analyzed the information in a given area of the visual field, that information is remembered and it is not necessary to analyze it again. This is equivalent to the hypothesis that the food doesn't grow back once it has been eaten.

\* \* \*

In this section, we want to check whether ARS emerges as an optimal solution to the foraging problem. We shall do this by implementing a genetic algorithm based on a competition among individuals whose characteristics are encoded in a string of bits called a *gene* [29].

Individuals move around a *foraging* areas under the guidance of their gene and collect food. Their *score*, which determines their fitness for survival, is the amount of food they have collected. The world in which these individuals move is a regular grid of patches of food of  $p \times p$  ( $p \in \mathbb{N}$ ) *pellets*, separated by barren areas without food (see Figure 26.9). Each pellet is

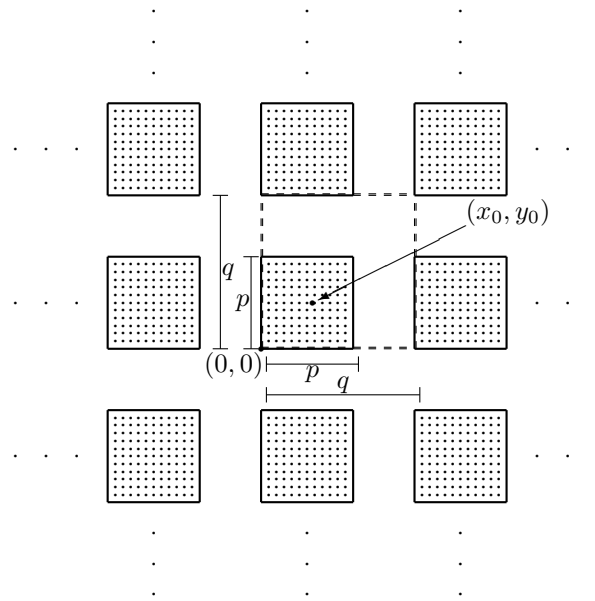


Figure 26.9: The environment for the application of genetic algorithms to the evolution of ARS. The dotted squares represent the patches composed of  $p \times p$  pellets of food, where  $p$  is a program parameter. The distance between the patches,  $q$ , is determined by the desired density of food,  $\rho$  (also a program parameter) through the relation  $q = \lceil p/\sqrt{\rho} \rceil$ . In the implementation, patches are generated dynamically the first time that the forager walks on them so that the foraging field is virtually infinite.

an atomic unit of food, that it, it is either not consumed or consumed entirely. The consumption of each pellet increases the survival fitness by one unit.

Each patch is separated from the other by being placed in the lower-left corner of a larger square of  $q \times q$  units ( $q \in \mathbb{N}$ ,  $q > p$ ) called a *plot*. The density of the food is  $\rho = p^2/q^2$ . The plots are created dynamically at run time as the walker steps on them for the first time, so that the foraging field is virtually infinite. In all the tests discussed below,  $p$  is kept fixed ( $p = 16$ ),  $\rho$  is a parameter that varies from  $\rho = 0.01$  to  $\rho = 0.95$ , and  $q$  is determined as  $q = \lceil p/\sqrt{\rho} \rceil$ . Each individual does a random walk (specified by certain parameters, as described below) starting at  $(x_0, y_0) = (p/2, p/2)$  that is, in the center of the patch whose lower-left corner is the origin.

### 26.2.1 The walk parameters

Each time the walker walks on a position containing a pellet, it "eats" it, incrementing its score (which determines its evolutionary fitness) by one. The pellet is removed, so that further visits to the location will not provide any food (Figure 26.10). The movement of each individual is a random walk whose statistical features depend on whether the individual is currently eating (status: on-food) or whether it has been without food for some time (status: off-food). The individual doesn't go "off-food" immediately as soon as it steps on a location with no food: the individual has memory, so that it gradually changes its status from on-food

to off-food during a certain number of time steps. The amount of time without food that it takes to go to the status off-food is controlled by a parameter in the gene of the individual. The general behavior of the random walk is the same regardless of whether the individual is

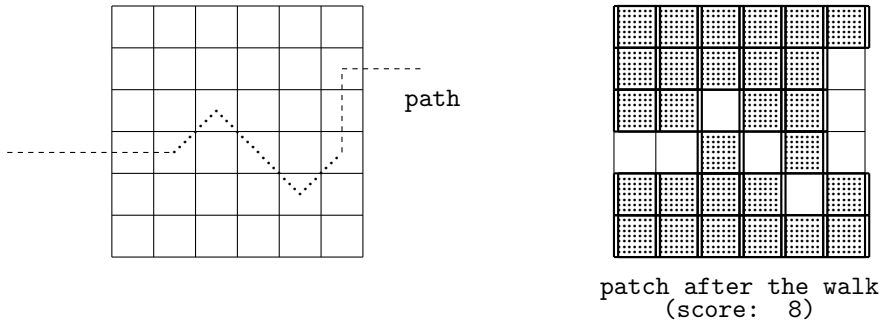


Figure 26.10: A walk of an individual through a patch of food: each square crossed by the individual is "eaten," and is removed from the patch. In this case, the individual passes over 8 patches: after the walk, its score is eight, and eight pellets are removed from the patch.

on-food or off-food (the only thing that changes in the two cases is the numerical value of the parameters). Consider a generic situation in which the parameters are  $(\alpha_0, l_0)$ . The individual is coming from a direction  $\theta$ , being currently at location  $(x, y)$ . The individual chooses a deviation angle  $\alpha$ , selected with a Gaussian distribution centered at  $\alpha_0$ , and a length  $l$  selected with an exponential distribution with average  $l_0$ , and performs a jump in a direction at an angle  $\alpha$  from its current direction, and for a length  $l$  (Figure 26.11). The parameters  $(\alpha_0, l_0)$  characterize the statistics of the jump, they are encoded in the individual's gene, and they take different values depending on whether the individual is on-food or off-food. When the individual is on-food, the jumps are done according to the parameters  $(\alpha_f, l_f)$ , while when the individual has been for some time off-food, the jumps are done according to  $(\alpha_n, l_n)$ . The switch from the on-food parameters to the off-food is done gradually when the individual is in an area without food. The gene defines a memory threshold  $\tau$  to switch from the on-food to the off-food behavior. If  $t$  is the number of step that the individual has been off-food ( $t = 0$  if the individual is on-food) then the parameters for the next jump will be

$$\begin{aligned}
 & (\alpha_f, l_f) && \text{on food} \\
 & \left. \begin{aligned}
 & (\alpha_f + \frac{t}{\tau}(\alpha_n - \alpha_f), l_f + \frac{t}{\tau}(l_n - l_f)) && t < \tau \\
 & (\alpha_n, l_n) && t \geq \tau
 \end{aligned} \right\} && \text{off food}
 \end{aligned} \tag{26.1}$$

The parameters of the jump are reset to  $(\alpha_f, l_f)$  as soon as the individual finds food. That is, there is a lingering memory that food was around there even if currently no food is found---a memory that fades away in a time  $\tau$ ---but the absence of food is forgotten as soon as new food is found. Any moral or philosophical conclusion, be it positive or negative, that can be drawn from this hypothesis is beyond the scope of these notes.

### 26.2.2 Gene definition

Each individual is therefore characterized by five parameters:  $(\alpha_f, l_f, \alpha_n, l_n, \tau)$ . We represent each one as a 8-bit value (these values are scaled in order to compute the actual values of the

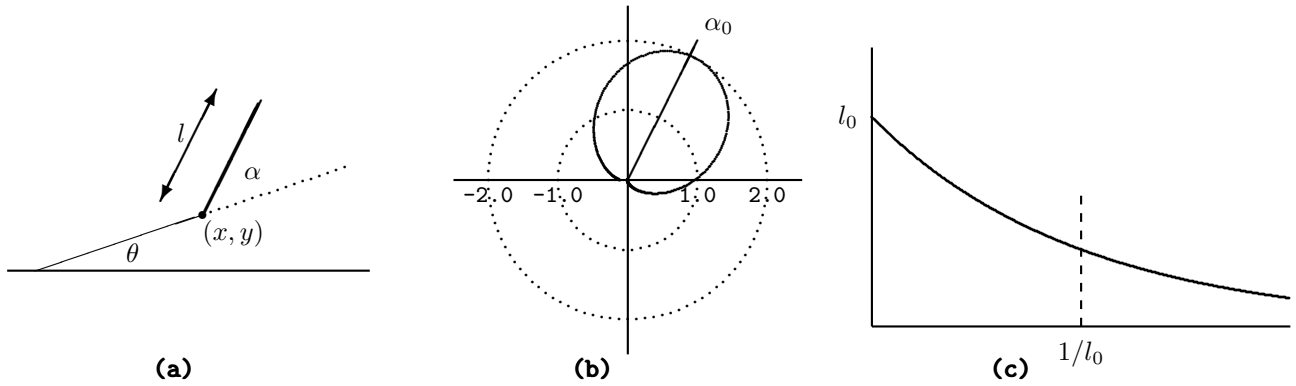


Figure 26.11: Generation of a single jump of the random walk. In (a), a walker is coming to point  $(x, y)$  following a trajectory with direction  $\theta$ . An angle  $\alpha$  is chosen from the Gaussian angle distribution in (b), centered around the angle  $\alpha_0$ : the direction of the new jump is  $\alpha$  from the previous direction (viz.  $\theta + \alpha$  absolute direction). The length of the jump is drawn from the exponential distribution with average  $l_0$  in (c).

parameters) and collect them in a 40-bit "gene." We try to keep related parameters in nearby positions of the gene (this is believed to speed up the convergence of the algorithm). Calling  $A_F$ ,  $L_F$ ,  $A_N$ ,  $L_N$ , and  $T$  the 8-bit representations of the parameters we have the genetic representation of an individual in Figure 26.12. The jump parameters are derived from these

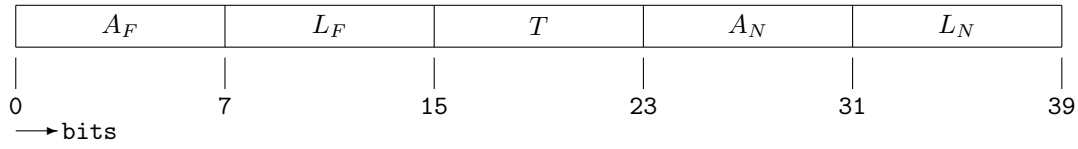


Figure 26.12: The genetic representation of an individual. The five 8-bit parameters are scaled to provide the jump parameters  $(\alpha_f, l_f, \alpha_n, l_n, \tau)$ .

8-bit integers as

$$\begin{aligned}
 \alpha_f &= 2\pi \frac{A_F}{256} & l_f &= \frac{L_F}{4} & \tau &= \frac{T}{10} \\
 \alpha_n &= 2\pi \frac{A_N}{256} & l_n &= \frac{L_N}{4}
 \end{aligned}
 \tag{26.2}$$

The scaling factors (except those for  $\alpha_f$  and  $\alpha_n$ , which are derived from geometric considerations) have been determined by trial and error.

### 26.2.3 The algorithm

The genetic algorithm is pretty standard. A *generation* is a set of individuals. Each individual is placed in the environment in the same initial position, and does a random walk of predetermined length, according to the parameters encoded in its gene, and collecting pellets of food as specified above. The environment is restored between individuals, so that each one has





$\delta$	$\alpha_f$	$l_f$	$\tau$	$\alpha_n$	$l_n$
0.95	0.00	136.94	57	34.25	33.50
0.5	199.06	15.53	0	2.00	60.50
0.1	309.18	1.75	18	285.18	58.00
0.01	227.29	1.50	37	345.88	45.50

Table 26.1: The values of  $A_F, L_F, T, A_N, L_F$  for the best individual for different values of the food density. The values are normalized as in (26.2) to obtain the walk parameters  $(\alpha_f, l_f, \tau, \alpha_n, l_n)$ .

Figure 26.13, in which we assume  $a < b$ . We also define a small mutation probability: for each new gene, with a (small) probability  $p$ , we pick a random bit and flip it. Note that this method doesn't guarantee that the best individual of a generation will pass unchanged to the next, so we actually use the crossing to create  $G - 2$  individuals to which we add the two best performers of the previous generation.

### 26.2.4 Results

Figure 26.14 shows typical paths from the best individual for various values of the density of food, while Table 26.1 shows the value of the parameters for the same individual. We note that in the case of high food density the random walk does not exhibit the characteristics of ARS (this observation will be made more formal later on), simply because the individual is always, or almost always, on food. As the density decreases, the behavior becomes more characteristic of ARS.

In order to study the characteristics of these walks, we consider the square average of the displacement from the initial position:

$$\langle X^2 \rangle \triangleq \langle (x - x_0)^2 + (y - y_0)^2 \rangle. \tag{26.3}$$

Let the individual be fixed (viz. let it be the best performing individual). We execute, with this individual,  $N$  random walks on the environment with the prescribed density, each of length  $T$ . Let

$$w^i = [p_0^i, \dots, p_t^i, \dots, p_T^i] \tag{26.4}$$

be the  $i$ th random walk, where  $p_t^i = (x_t^i - x_0, y_t^i - y_0)$ . We are interested in knowing how far the individual has gone, on average, from its initial position, at time  $t$ . That is, we are interested in studying the function

$$\langle X^2(t) \rangle = \frac{1}{N} \sum_{i=1}^N (p_t^i)^2 \tag{26.5}$$

Figure 26.15 shows the behavior of  $\langle X^2(t) \rangle$  as a function of  $t$  for various values of the density  $\rho$ , together with the best approximation of the form  $\langle X^2(t) \rangle \sim x^\nu$ , where the exponent  $\nu$  depends on  $\rho$ :

$\rho$	0.01	0.1	0.5	0.9
$\nu$	3.78	1.8	1.1	0.95

Figure 26.16 shows the behavior of the exponent  $\nu$  as a function of  $\rho$ . As density approaches 1 or 0, that is, as the environment becomes more homogeneous (either with a lot of food or very

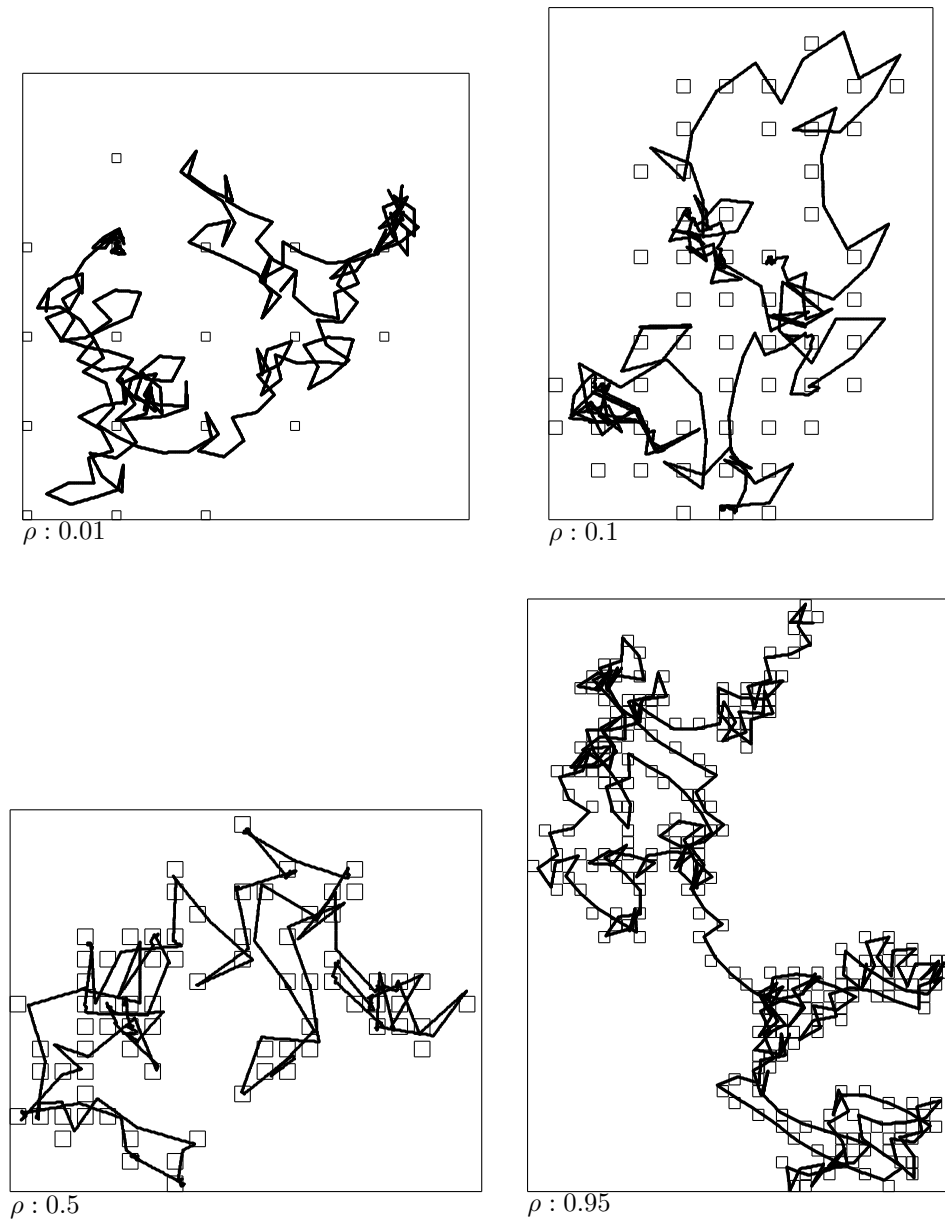


Figure 26.14: A typical path of the best individual for various values of the density. Note the different macroscopic behavior for high density and for low density. In the case of high density, the path is practically always contained in some patch, and the off-food status is practically unused. The low density situation shows the characteristics of ARS.

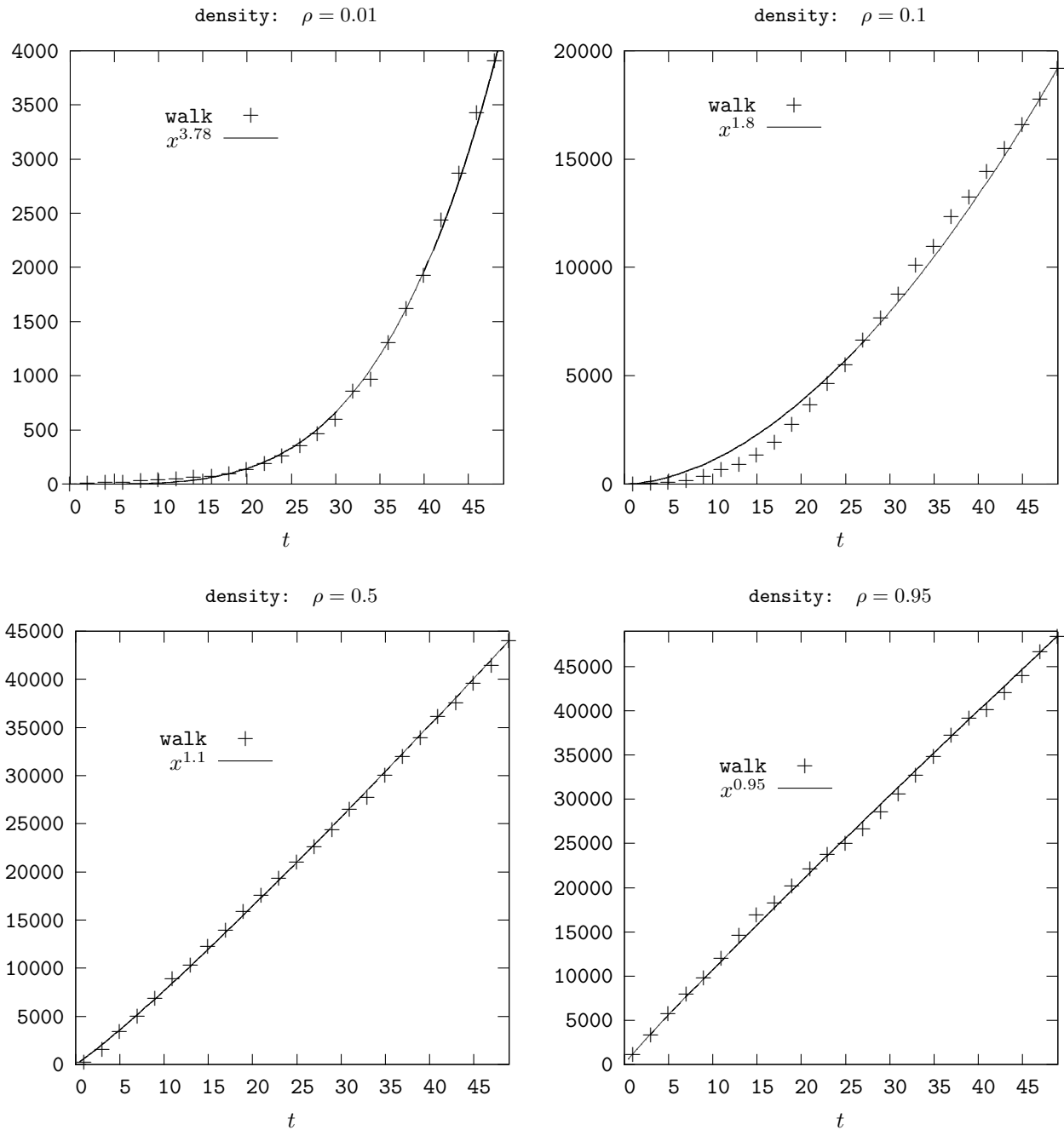


Figure 26.15: The behavior of  $\langle X^2(t) \rangle$  as a function of  $t$  for various values of the resource density  $\rho$ . Together with the curve, the figure shows its best approximation as  $\langle X^2(t) \rangle \sim x^\nu$ . The coefficient  $\nu$  of the best approximation varies with  $\rho$ . On the significance of this variation, see the text.

little food), the exponent approaches 1, that is, we approach a situation in which  $\langle X^2(t) \rangle \sim x^1$ . This, as we shall see, is the behavior characteristic of Brownian motion, as well as of several other types of random walks. This should not come as a surprise: when food can be found everywhere, the individuals have no particular reason to modify their behavior, and will simply move to and fro in an haphazard manner: they will do a random walk. The same is true if there is very little food. The patches are so small and far apart that the in-patch behavior will last for a very short time and will not change significantly the characteristics of the walk, which will be a random walk from patch to patch looking for resources.

When the food is patchy, on the other hand, the random walk of the individual doesn't follow the standard Brownian model. In the next section I shall consider the foraging walk more closely from a mathematical point of view. We shall begin, in the next section by considering the switching from the on-patch behavior to the off-patch, without taking into account the spatial characteristics of the environment. Then, in the following section, we shall study random walks in search of a model that fits the characteristics of a forager on patchy resources. We shall see that such a model is given by the so-called Levy walks.

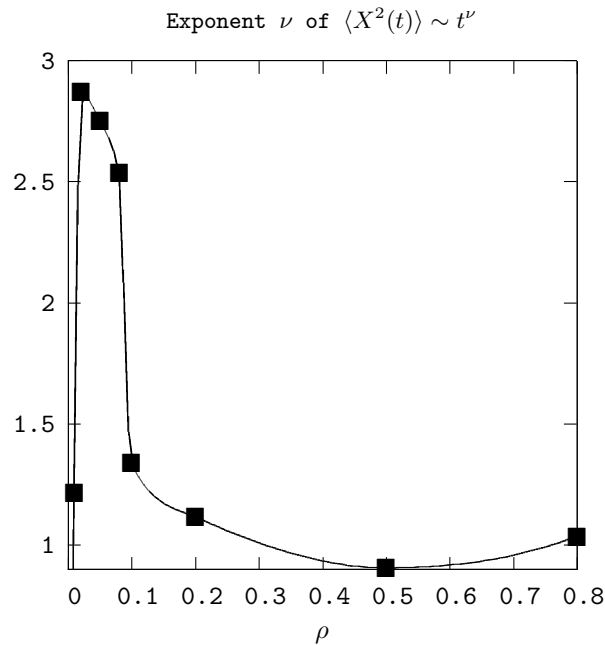


Figure 26.16: Exponent of the best approximation  $\langle X^2(t) \rangle \sim x^\nu$  as a function of  $\rho$ . The squares are the values that have been calculated from the simulation (in each case the best gene as resulting from the genetic algorithm has been used), the continuous line is a spline interpolation [34]. The value  $\nu \sim 1$  is characteristic of standard Brownian motion. For very low and high  $\rho$ , the walk is essentially Brownian: when the density is very low, the forager wanders long distances and spends comparatively little time on each patch. When  $\rho \sim 1$ , there is no ARS, as the food is everywhere. The region  $0.1 < \rho < 0.4$  is that in which ARS is clearly taking place.

### 26.3 SHOULD I STAY OF SHOULD I GO?

In the next section, I shall analyze the global characteristics of ARS exploration considering it as a random walk such as those that emerge from our genetic experiment. Before that, in this section I shall consider a more basic problem. Suppose that you are in a patch. For a while, you stay there happily eating, as there is plenty of food. After a while, the food begins to dwindle, the resources of the patch begin to be exhausted. When is it a good time to leave? You are confronted with two contrasting criteria. On the one hand, staying implies that you can continue eating without having to make a possibly long journey without food before you find another patch. In the long run, you want to spend more time in a patch and less between patches. On the other hand, the new patch that you will find has lots and lots of food so it might be a good idea for you to move now to greener pastures instead of half starving in this half barren patch. When is it a good time to leave? This is the question I want to answer in this section. I shall consider a very simple model: I analyze only the time that an individual spends on a patch ( $t_p$ ) and the time that it spends between patches ( $t_b$ ), and how to optimize them for maximum foraging efficiency. In this, I follow essentially the techniques developed for *optimal foraging theory* [41].

Suppose that a forager searches for food for a certain (long) amount of time. It spends a total time  $T_b$  looking for the next patch, and a total time  $T_p$  staying on a patch and eating (all the symbols used in this section are shown in Table 26.2) If the total gain of the activity is  $G$ ,

Symbol	Meaning
$T_b$	Total time spent looking for a patch,
$T_p$	total time spent on a patch,
$t_b$	average time spent looking for a patch,
$t_p$	average time spent on a patch,
$G$	total resource gain,
$g$	average gain per patch,
$g(t)$	gain per patch as a function of the time spent on a patch,
$R$	rate of reward: average gain per time unit,
$\pi$	$= g/t_p$ , profitability of a patch (resource per unit time when on the patch),
$\lambda$	average number of patches found per unit time,
$P$	number of types of patches,
$p_i$	probability of using a resource of type $i$ .

Table 26.2: Symbols used in this section.

then the rate of reward (reward per unit time), is

$$R = \frac{G}{T_b + T_p} \tag{26.6}$$

This equation is inconvenient as it depends on the total times  $T_p$  and  $T_b$  and on the total gain  $G$  (if the time spent goes to infinity, both the numerator and the denominator go to infinity). One can derive a more convenient equation, independent on the actual foraging time, by considering the average on-patch time  $t_p$ , the average time between patches  $t_b$  and the average gain per patch  $g$ . The rate at which patches are discovered, that is, the number of patches

discovered per unit time, is  $\lambda = 1/t_b$ . The total number of patches discovered during foraging is therefore  $\lambda T_b$ . The total gain and the total time spent on patches depend on this number, that is:

$$\begin{aligned} G &= \lambda T_b g \\ T_p &= \lambda T_b t_p \end{aligned} \quad (26.7)$$

Introducing these values in (26.6) we have

$$R = \frac{\lambda T_b g}{T_b + \lambda T_b t_p} = \frac{\lambda g}{1 + \lambda t_p} \quad (26.8)$$

or, in terms of average times

$$R = \frac{g/t_b}{1 + t_p/t_b} = \frac{g}{t_b + t_p} \quad (26.9)$$

This equation is known as the *Holling disk equation* [25]<sup>2</sup>. Define the profitability of a patch as  $\pi = g/t_p$ , that is, the gain per unit of time spent on the patch. With this definition we have:

$$R = \frac{\pi}{1 + \frac{t_b}{t_p}} \quad (26.10)$$

When the patches become more and more dense, then  $t_b \rightarrow 0$ , and

$$\lim_{t_b \rightarrow 0} \frac{\pi}{1 + \frac{t_b}{t_p}} = \pi \quad (26.11)$$

This simple model can be extended in several ways. One very useful one is to consider that a patch has *diminishing returns*: as the forager spends time on a path, its resources become depleted, so it becomes harder to get rewards, and the profitability of the patch is reduced.

That is, the reward  $g$  is a function of  $t$ ,  $g(t)$ , that tells us how much reward one accumulates while foraging on a patch for a time equal to  $t$ . The profitability is also a function of time:  $\pi(t) = g(t)/t$ . Physical considerations place certain constraints on these functions. The gain is positive and cumulative (you never lose what you have gained), which implies  $g(t) \geq 0$  and  $g'(t) \geq 0$ . The first inequality also entails  $\pi(t) \geq 0$ . On the other hand, it is reasonable to assume that, as time goes by and the resources become depleted, it will take longer and longer to amass the same amount of reward; this entails  $\pi'(t) \leq 0$ . These two relations imply  $\lim_{t \rightarrow \infty} \pi(t) = C \geq 0$ . The condition  $\pi'(t) \leq 0$  imposes conditions on  $g'(t)$ . From  $\pi(t) = g(t)/t$ , we have

$$\pi'(t) = \frac{1}{t^2} [g'(t)t - g(t)] \leq 0 \quad (26.12)$$

that is

$$g'(t) \leq \frac{g(t)}{t} = \pi(t) \quad (26.13)$$

I assume certain regularity conditions. In particular, that  $\pi(t)$  decreases without "bumps", that is, that  $\pi'$  is monotonically increasing, which entails that  $\pi'' \geq 0$ . Similarly, I assume  $g''(t) \leq 0$ . Note that in the most common case the patch will become depleted, that is,

$$\lim_{t \rightarrow \infty} g(t) = g_\infty > 0 \quad (26.14)$$

---

<sup>2</sup>The name "disk equation" has nothing to do with the properties of the equation. Holling developed his model by studying the behavior of a blindfolded researcher assistant who was given the task of picking up randomly scattered sandpaper disks.

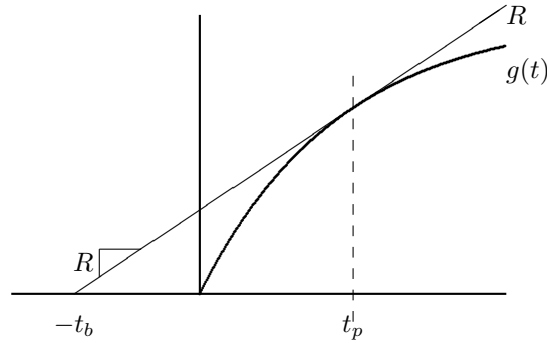


Figure 26.17: A graphical illustration of Charnov’s Marginal Value Theorem. The patch time  $t_w$  that maximizes the rate of gain  $R$  occurs when the line with slope  $R$  is tangent to the function  $g(t)$ , that is, when the instantaneous rate of gain on the patch equals the average rate of gain  $R$ .

but the analysis applies to the more general case in which  $g(t)$  goes to infinity slower than a linear function.

Given the average between-patches time  $t_b$ , we are interested in finding the optimal time that the forager should spend on a patch ( $t_p$ ) to maximize the reward  $R$ . The idea is that if you spend too little time on a patch, then you don’t take full advantage of its resources, and spend comparatively too much time without patches, in an area where you have no reward: your rate of gain will be reduced.

On the other hand, since the resources get depleted as we stay on a patch, if you spend too much time there you shall waste your time on a depleted patch that won’t yield too much, while it would be more convenient to invest some time ( $t_b$ ) to find a new patch with better yield. Given the equality

$$R(t) = \frac{g(t)}{t_b + t} \tag{26.15}$$

compute the derivative

$$\frac{\partial R}{\partial t} = \frac{g'(t)(t_b + t) - g(t)}{(t_b + t)^2} \tag{26.16}$$

It is  $\partial R/\partial t = 0$  if  $g'(t)(t_b + t) - g(t) = 0$ , that is, if

$$g'(t) = \frac{g(t)}{t_b + t} = R \tag{26.17}$$

This result is known as the *Charnov’s Marginal Value Theorem* [8].

This equation has a simple geometric interpretation. The average gain  $R$  results in a straight line in a  $t$ - $g$  diagram (Figure 26.17). The patch gain is a curve that stays at zero for a time  $t_b$  and then grows as  $g(t)$ ; the optimal  $t_p$  occurs when the slope of the curve  $g(t)$  is equal to the average rate of gain. Note that there are two ways in which the environment can change so that  $R$  increases. First, the profitability of the patch may increase, that is, the curve  $g(t)$  can be pulled upward (Figure 26.18.a). Second, the patches may become dense, reducing  $t_b$  (Figure 26.18.b). As  $t_b \rightarrow 0$  the rate  $R$  approaches  $\pi$  (the profitability of the patch), as per (26.11).

**Example I:**

Suppose we are looking for a low-priced hotel in Paris. We have several web sites available, and our strategy is to log in to one, start checking prices looking for the cheapest price for a

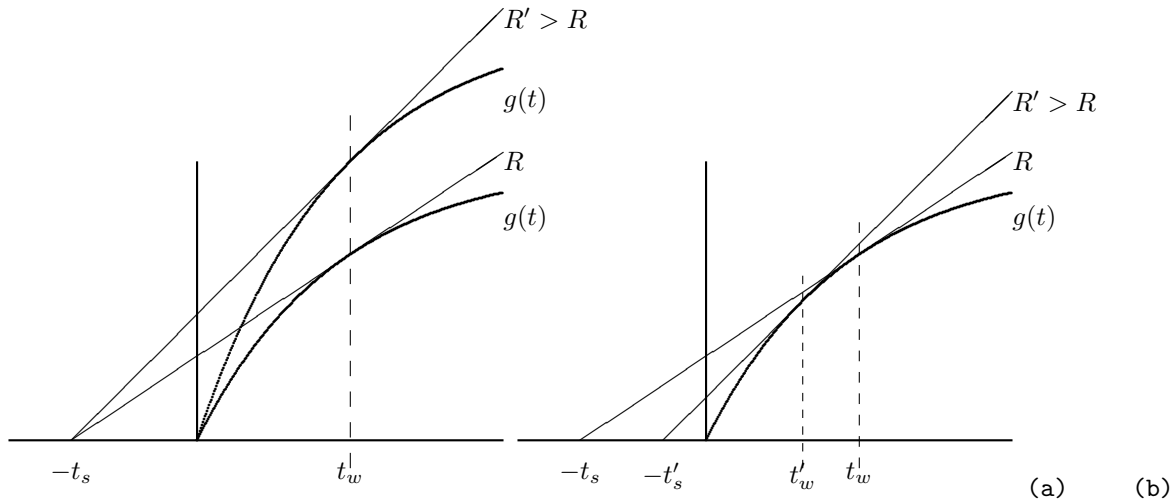


Figure 26.18: As a consequence of Charnov's Marginal Value Theorem, there are two ways to increase the average rate of gain  $R$ : one can either increase the profitability of a patch, i.e. raising the gain curve  $g(t)$  as in (a), or make the patches more dense, thereby decreasing the average between-patches time  $t_b$ , as in (b).

while, then move to another one looking for a new price or, simply, stop looking and accept the lowest price we have found. The question is: how long should we stay on the site and keep looking before we move on?

When we are on a page, the important events are the prices that we look at so, for the sake of convenience, we take the time that it takes to move from one hotel to the next one on the same page as the time unit so that at time  $t = n$  we have looked at  $n + 1$  prices (we look at the first price at  $t = 0$ ). The actual length depends of what we are looking for: if we look just for the best price, the interval is very small; if we look for price subject to certain constraint (hotel with a bar, with a sauna, etc.), it will take longer. In any case, we look at a new hotel (one the same page) per unit of time. In these units, let  $t_b$  be the time that it takes to get set on a page (including typing the address, logging in, etc.)

We begin by determining the expected value of the minimum price that we have observed if we have observed  $n$  prices. In this simple example we shall favor simplicity over plausibility and we shall assume that the prices of the hotels are uniformly distributed in the interval  $[\mu - a, \mu + a]$ .

To begin with, we shall answer an even simpler question: given  $n$  observations  $X = \{x_1, \dots, x_n\}$  of  $n$  random variables independent and uniformly distributed in  $[-1, 1]$ , which is the expected value of  $\min(X)$ ? The cumulative distribution and the density for each of the  $x_i$  are

$$\Phi(x) = \begin{cases} 0 & x \leq -1 \\ \frac{x+1}{2} & -1 < x < 1 \\ 1 & x \geq 1 \end{cases} \tag{26.18}$$

and

$$\phi(x) = \begin{cases} \frac{1}{2} & -1 \leq x \leq 1 \\ 0 & \text{otherwise} \end{cases} \tag{26.19}$$



respectively. The probability density for the minimum is given by (A.82):

$$\phi_{\min}(x) = n[1 - \Phi(x)]^{n-1}\phi(x) = \begin{cases} \frac{n}{2^n}[1 - x]^{n-1} & (-1 \leq x \leq 1) \\ 0 & \text{otherwise} \end{cases} \quad (26.20)$$

and its expected value is

$$\begin{aligned} m(n) &= \int_{-1}^1 u\phi_{\min}(u)du = \frac{n}{2^n} \int_{-1}^1 u(1-u)^{n-1}du \\ &= \frac{n}{2^n} \left[ \int_{-1}^1 (1-u)^{n-1}du - \int_{-1}^1 (1-u)^n du \right] \\ &= \frac{n}{2^n} \left[ -\int_2^0 u^{n-1}du + \int_2^0 u^n du \right] \\ &= \frac{n}{2^n} \left[ \frac{2^n}{n} - \frac{2^{n+1}}{n+1} \right] \\ &= \frac{1-n}{1+n} \end{aligned} \quad (26.21)$$

Scaling and shifting one obtains, for variables distributed in  $[\mu - a, \mu + a]$ :

$$m(n) = \mu - a \frac{1-n}{1+n} \quad (26.22)$$

Note that if we only observe one price, the expected value of the minimum is  $\mu$ . We observe more prices, the expected value decreases, with

$$\lim_{t \rightarrow \infty} m(t) = \mu - a \quad (26.23)$$

Let us consider that we start exploring at the time when we observe the first price, and that everything that comes before that is preparation that is included in the time  $t_b$ . At time  $t$ , we have looked at  $t+1$  prices, and the expected value for the minimum price is  $m(t+1)$ . The gain that we have obtained is the difference between the first price that we saw (expected value equal to  $\mu$ ) and the current one:

$$g(t) = m(1) - m(t+1) = a \frac{t}{t+2} \quad (26.24)$$

Up to now, I have considered  $t$  as a discrete variable (the number of prices observed); from now on we regard it as a continuous variable, so I can take the derivative:

$$g'(t) = \frac{2a}{(t+2)^2} \quad (26.25)$$

I now apply Charnov's Marginal value theorem: the optimal value to spend on the site is given by

$$g'(t) = \frac{2a}{(t+2)^2} = \frac{at}{t+2} \frac{1}{t+t_b} = \frac{g(t)}{t+t_b} \quad (26.26)$$

which has solution  $\tau_1 = \sqrt{2t_b^3}$ . The corresponding rate of reward is

$$R_1 = g'(\tau_1) = \frac{2a}{(\sqrt{2t_b} + 2)^2} = \frac{a}{(\sqrt{t_b} + \sqrt{2})^2}. \quad (26.27)$$

---

<sup>3</sup>Dimensionally, the equation is sound: the factor  $t + 2$  in (26.24) entails that the term 2 has the dimensions of a time.

Note that the time that we spend on a site grown sub-linearly with the time we spend looking for the site: if we spend twice as long looking for the web page, the time we should spend on the web page grows like  $\sqrt{2}$ , that is, we should stay about 40% longer.

(end of example)

**Example II:**

The considerations of the previous example are valid for the first "patch", that is, for the first site that we visit. Suppose now that we want to visit a second site (the time necessary to do the switch is assumed to be  $t_b$ ). Now we already have a minimum, the one that we found in the first patch, namely

$$m_1 \triangleq \mu - a \frac{\tau_1}{\tau_1 + 2} = \mu - a \frac{\sqrt{t_b}}{\sqrt{t_b} + \sqrt{2}} \triangleq \mu - a\alpha \quad (26.28)$$

with

$$\alpha \triangleq \frac{\sqrt{t_b}}{\sqrt{t_b} + \sqrt{2}} < 1 \quad (26.29)$$

While we explore the second site, as long as the minimum price that we find there is greater than  $m_1$ , our gain is zero. Assume that the second patch has the same average price as the first, but a larger spread, that is, in the second patch the prices are uniformly distributed in  $[\mu - b, \mu + b]$ , with  $b > a$ . Also, define  $\gamma = b/a > 1$  (I shall need it later).

The current minimum after we have explored the second site for a time  $t$  is

$$\tilde{m}(t) = \mu - b \frac{t}{t + 2} \quad (26.30)$$

The expected minimum in the second site is the same as the optimal price in the first at a time  $t_0$  such that  $\tilde{m}(t_0) = m_1$ , that is

$$t_0 = \frac{2a\alpha}{b - a\alpha} = \frac{2\alpha}{\gamma - \alpha} \quad (26.31)$$

The gain in the second site is given by the savings we obtain over the previous minimum, that is

$$g_2(t) = \begin{cases} 0 & t < t_0 \\ b \frac{t}{t+2} - a\alpha & t \geq t_0 \end{cases} \quad (26.32)$$

and

$$g_2'(t) = \begin{cases} 0 & t < t_0 \\ b \frac{2b}{(t+2)^2} - a\alpha & t \geq t_0 \end{cases} \quad (26.33)$$

The situation is depicted schematically in figure 26.19. When we arrive at the second site, a time  $T \triangleq 2t_b + \tau_1$  has already elapsed, so if we stay on the site a time  $\tau$ , the rate of gain is:

$$R_2(\tau) = \frac{g_2(\tau)}{T + \tau} = \frac{g_2(\tau)}{2t_b + \tau_1 + \tau} \quad (26.34)$$

To find the maximum of  $R_2(\tau)$  we proceed as in the previous example, setting

$$g_2'(\tau) = \frac{g_2(\tau)}{T + \tau} \quad (26.35)$$

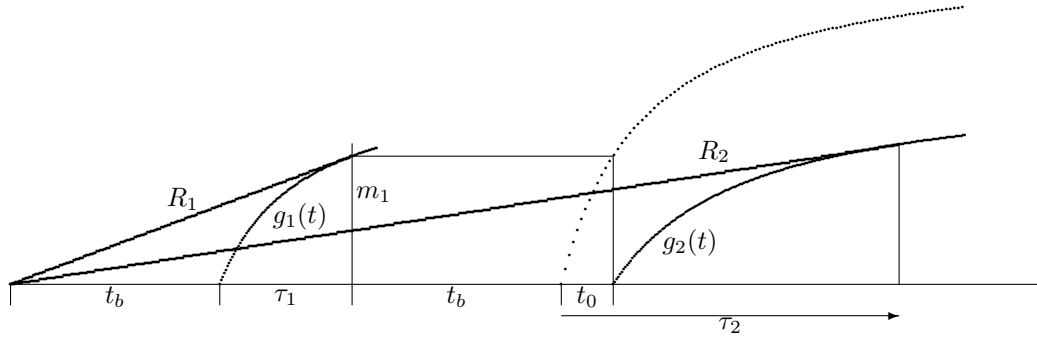


Figure 26.19: A graphical illustration of the Charnov's Marginal Value Theorem for two sites. When we get to the second site, we already have a minimum  $m_1$  from the first site so that the gain  $g_2(t)$  only is greater than zero starting from  $t_0$ . The second patch has prices distributed in  $[\mu - b, \mu + b]$ : for a large enough value of  $\gamma = b/a$  the rate of gain  $R_2$  that we obtain by exploring the second site is greater than the rate  $R_1$  obtained in the first site.

that is

$$\frac{2b}{(\tau + 2)^2} = \frac{1}{T + \tau} \left[ \frac{\tau b}{\tau + 2} - a\alpha \right] \tag{26.36}$$

or

$$\frac{2}{(\tau + 2)^2} = \frac{1}{T + \tau} \left[ \frac{\tau}{\tau + 2} - \frac{\alpha}{\gamma} \right] \tag{26.37}$$

that is

$$2(T + \tau) = (\tau + 2) \left[ \tau - \frac{\alpha}{\gamma}(\tau + 2) \right] \tag{26.38}$$

Rearranging the terms, we obtain the equation

$$(\gamma - \alpha)\tau^2 - 4\alpha\tau - (4\alpha + 2\gamma T) = 0 \tag{26.39}$$

whose only positive solution is given by

$$\begin{cases} \Delta = 8\gamma [2\alpha + (\gamma - \alpha)T] \\ \tau_2 = \frac{4\alpha + \sqrt{\Delta}}{2(\gamma - \alpha)} \end{cases} \tag{26.40}$$

The corresponding maximum rate of gain is

$$R_2 = g_2'(\tau_2) = \frac{2b}{(\tau_2 + 2)^2} \tag{26.41}$$

Using the second patch is convenient if we improve our gain rate, that is, if  $R_2 > R_1$ , where  $R_1$  is as in (26.27). This imposes a condition on  $b/a$ , that is, on  $\gamma$ : it is convenient to use the second patch if  $\gamma$  is large enough that we can find a better price that offsets the extra time spent in searching. The limit condition  $R_2 = R_1$  yields

$$\gamma = \left[ \frac{\tau_2 + 2}{\sqrt{2t_b} + 2} \right]^2 \tag{26.42}$$

The value of  $\tau_2$  depends on  $\gamma$  in such a way that we can't find a closed form solution to this equation. We can, however, determine its limits. For  $t_b \rightarrow 0$ , we have  $\alpha \rightarrow 0$ ,  $T \rightarrow 0$ ,  $\Delta \rightarrow 0$ , and  $\tau_2 \rightarrow 0$ , therefore

$$\lim_{t_b \rightarrow 0} \gamma = 1 \tag{26.43}$$

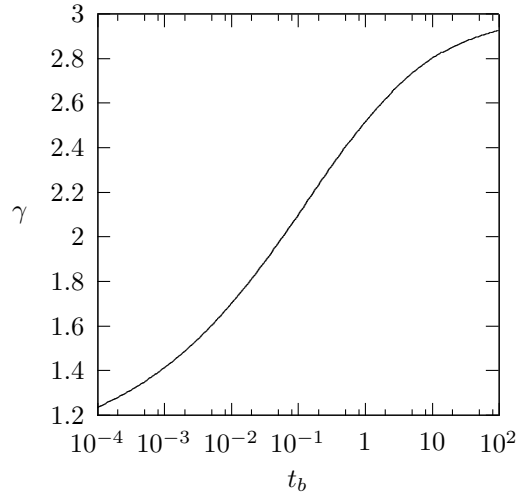


Figure 26.20: The behavior of  $\gamma$  as a function of  $t_b$  (the horizontal axis is logarithmic). For a given  $t_b$ , if the ratio of the spreads of the two patches,  $b/a$  is greater than the  $\gamma$  shown in this graph, then it is convenient to explore the second patch.

For  $t_b \rightarrow \infty$ ,  $\alpha \rightarrow 1$ ,  $T \sim 2t_b$ , and

$$\begin{aligned} \Delta &\sim 16\gamma(\gamma - 1)t_b \\ \tau &\sim 2 \frac{\sqrt{\gamma(\gamma - 1)}}{\gamma - 1} \sqrt{t_b} \end{aligned} \quad (26.44)$$

The equation

$$\gamma = \left[ \frac{2\sqrt{\gamma(\gamma - 1)}}{\sqrt{2}(\gamma - 1)} \right]^2 = \frac{2\gamma}{\gamma - 1} \quad (26.45)$$

has solution  $\gamma = 3$ , therefore

$$\lim_{t_b \rightarrow \infty} \gamma = 3 \quad (26.46)$$

The behavior of  $\gamma$  can be found solving (26.45) numerically, which, given the stability of the equation, can be done with a simple iteration. The result is shown in figure 26.20 For  $\frac{b}{a} > \gamma(t_b)$  and switch time  $t_b$ , it is convenient to explore the second patch.

## 26.4 WALKING IN CONTINUOUS SPACE

We have seen, in the first section, the neurological basis of ARS, and its widespread presence to solve many apparently unrelated problems in the animal kingdom. All these problems have a common abstract structure: that of foraging in a patchy environment, that is, in an environment in which the resources are distributed in clumps: there are concentrated areas in which the resource is present, separated by stretches in which no (or little) resource is found.

Some fiddling with genetic algorithms convinced us that ARS is indeed an optimal strategy for this kind of problems. The problem that I should like to consider now is how to characterize

Input	Description Level	Output	Math, formalism	↑ complexity
individual fluctuations	microscopic	trajectories	Langevin equations	
averaged fluctuations	mesoscopic	prob. density	Master equation	
macroscopic parameters	macroscopic	prob. density	Fokker-Planck equations	

Figure 26.21: Three levels of description of random walks: the mesoscopic entails considering the time span of each motion small with respect to the time of the whole phenomenon, and approximating time functions with their first derivatives; the macroscopic entails making the same approximation on space. This entails that the master equation (mesoscopic) is a differential equation in time and an integral equation in space, while the Fokker-Planck equation (macroscopic) is differential in time and space. (Adapted from [28].)

this behavior at a large scale. I have shown in the previous section how to decide when to leave a patch and venture in search of another, now I am interested in analyzing the global behavior that results from these decisions. One result, which we have already glimpsed at the end of section 26.2 is to see ARS as a type of *random walk*. In this section, we shall study the paths produced by ARS as random walks in a continuum (viz. in  $\mathbb{R}^n$ , usually in  $\mathbb{R}^2$ ). As we shall see, an important parameter in this exploration is the exponent  $\nu$  of the curves in Figure 26.15, that is, in the relation  $\langle X^2(t) \rangle \sim t^\nu$ ; the fact that  $\nu > 1$  makes ARS walk of a peculiar kind, known as *Levy walks*.

### 26.4.1 Random Walks and Diffusion Processes

A random walk is the description of the motion of a point (sometimes called, in reference to the physics in which random walks were first studied, a *particle* or, in reference to ecology, an *individual*) subject to forces that can be modeled as a stochastic process. Random walks can be described at three levels of detail, given by the schema of Figure 26.21). We shall consider these levels of description one by one, especially as they apply to the best known model of random walk: *Brownian motion*.

### 26.4.2 Microscopic description--Langevin equations

Langevin's equations were originally studied for what become the prototype of diffusive random walks, namely *Brownian motion* [22, 27]. In 1827, botanist R. Brown discovered, during microscopic observations, that particles of pollen suspended in water exhibited an incessant and irregular motion [33]. Vitalist explanations were soon discarded since mineral (viz. non-living) particles exhibited the same phenomenon. Brownian motion occurs when the mass of the particle of pollen is larger than the mass of the molecules of the liquid, so that the continuous collisions drive the particles in a chaotic way (Figure 26.22). The first theoretical explanation of this phenomenon was given in 1905 by Albert Einstein at a macroscopic level [15], and we shall consider his approach shortly. In 1906, Paul Langevin offered a microscopic model of Brownian motion based on stochastic differential equations. Langevin's

equations for a one-dimensional Brownian motion (the case that is commonly studied) are:

$$\begin{aligned}\frac{dx}{dt} &= v \\ m\frac{dv}{dt} &= -\gamma v + \sigma\xi(t)\end{aligned}\tag{26.47}$$

where  $m$  is the particle mass,  $\gamma$  is the friction coefficient, and  $\xi(t)$  is the force resulting from the impact with the molecules. Langevin assumed that  $\xi(t)$  is a Gaussian, uncorrelated stochastic process with zero mean, that is  $\langle\xi(t)\rangle = 0$ ,  $\langle\xi(t)\xi(t')\rangle = \delta(t-t')$ . He also considered the limit of strong friction  $m|dv/dt| \ll |\gamma v|$  (more on this hypothesis later) so the equations become

$$\gamma\frac{dx}{dt} = \sigma\xi(t)\tag{26.48}$$

and, defining the *diffusion coefficient*  $D = \frac{\sigma^2}{2\gamma^2}$ ,

$$\frac{dx}{dt} = \sqrt{2D}\xi(t)\tag{26.49}$$

or

$$dx = \sqrt{2D}\xi(t)dt = \sqrt{2D}dW(t)\tag{26.50}$$

where  $W(t)$  is a Wiener process (see section A.1.5). Integrating (26.50) we get

$$x(t) = x(0) + \sqrt{2D}w(t)\tag{26.51}$$

So, Brownian motion is the motion of a particle whose displacement is a Wiener process and whose velocity is an uncorrelated Gaussian process. The hypothesis of strong friction is key to obtain velocity as an uncorrelated stochastic process: if inertial phenomena are present, then the velocities at two different instants in time are correlated.

From the solution of this equation we can determine macroscopic quantities such as the mean position  $\langle X \rangle$  and the mean square displacement  $\langle X^2 \rangle - \langle X \rangle^2$ :

$$\begin{aligned}\langle X \rangle &= \langle X(0) \rangle + \sqrt{2D}\langle W(t) \rangle = \langle X(0) \rangle \\ \langle X^2 \rangle - \langle X \rangle^2 &= 2D\langle W^2(t) \rangle = 2Dt\end{aligned}\tag{26.52}$$

From the second equation we see that  $\langle X^2 \rangle \sim t$ . This is an equation that we have already encountered: it characterizes the ARS walk for very low  $\rho$  and for  $\rho \sim 1$  (figure 26.15). It is a behavior typical of *diffusive processes*, and we shall meet it quite a few times in the following.

### 26.4.3 Mesoscopic description--Master equation

The *master equation* is an ensemble equation that expresses the probability  $P(x, t)$  that a particle be at position  $x$  at time  $t$ . It is an integro-differential equation, expressing the time derivative of  $P(x, t)$  as a balance of the probability of arriving at  $x$  and the probability of leaving the position  $x$  once we are there.

Consider a stationary Markov process. For this kind of process, the probability  $P(x, t|z, t')$  depends only on  $t - t'$ , so we can define  $P_\tau(x, z) = P(x, t + \tau|z, t) = P(x, \tau|z, 0)$ .

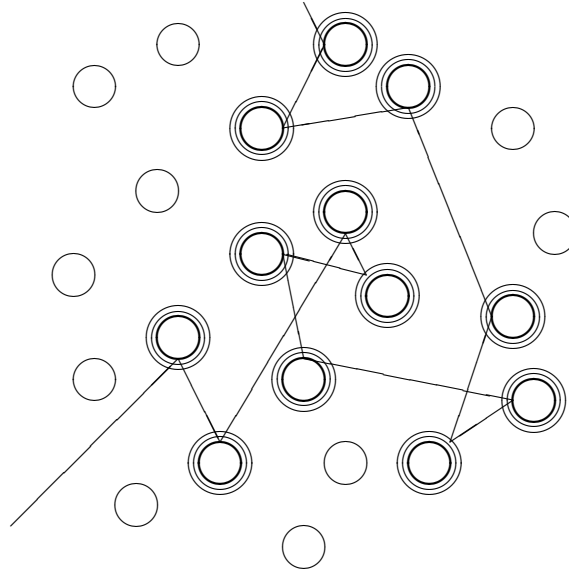


Figure 26.22: A schematic illustration of Brownian motion: a particle of pollen "bumps" on the molecules of the liquid in which it is suspended, creating an irregular random trajectory.

Consider now  $P(x, t + \tau)$ , that is, the probability that the walking particle will be in position  $x$  at time  $t + \tau$ . The particle is in  $x$  at time  $t + \tau$  if there is a position  $z$  such that the particle was in  $z$  at time  $t$  and has moved from  $z$  to  $x$  in the time interval  $\tau$  (if  $z = x$ , this is the probability that the particle were already in  $x$  and hasn't moved). This event, for a specific  $z$ , has a probability  $P(z, t)P_\tau(x, z)$ . Integrating over all possible  $z$ , we obtain

$$P(x, t + \tau) = \int_{-\infty}^{\infty} P(z, t)P_\tau(x, z) dz \tag{26.53}$$

If  $\tau \ll t$ , we can approximate  $P(x, t + \tau)$  as

$$P(x, t + \tau) = P(x, t) + \frac{\partial P}{\partial t} \tau + O(\tau^2) \tag{26.54}$$

Let  $\omega(x|z)$  be the transition probability per unit time from  $z$  to  $x$ , that is,  $\omega(x|z)\tau$  is the probability that the particle go from  $z$  to  $x$  in a time  $\tau$ . If the particle is in  $x$  at time  $t$ , then

$$\int_{-\infty}^{\infty} \omega(z|x)\tau dz \tag{26.55}$$

is the probability that it will move somewhere else, and

$$1 - \int_{-\infty}^{\infty} \omega(z|x)\tau dz \tag{26.56}$$

is the probability that it will stay in  $x$ . Balancing the probability of arriving at  $x$  and that of not moving if we are already there, we obtain

$$P(x, t + \tau) = P(x, t) \left( 1 - \int_{-\infty}^{\infty} \omega(z|x)\tau dz \right) + \int_{-\infty}^{\infty} \omega(x|z)P(z, t)\tau dz \tag{26.57}$$

The first terms gives us the probability that the particle were in  $x$  at time  $t$  and did not move in the interval  $[t, t + \tau]$ , while the second is the probability that the particle were in a different position at  $t$  and that it moved to  $x$  in the interval  $[t, t + \tau]$ . Rearranging and taking the limit for  $\tau \rightarrow 0$ , we obtain the *master equation*

$$\frac{\partial}{\partial t} P(x, t) = \int_{-\infty}^{\infty} \omega(x|z) P(z, t) dz - \int_{-\infty}^{\infty} \omega(z|x) P(x, t) \tau dz \quad (26.58)$$

If  $X$  is a discrete stochastic process, then, calling  $\omega_{nm}$  the prbability of moving from position  $x_n$  to position  $x_m$  in unit time, the equation becomes

$$\frac{\partial}{\partial t} P(n, t) = \sum_m \omega_{mn} P(m, t) - \sum_m \omega_{nm} P(n, t) \quad (26.59)$$

(end of example)

**Example III:**

As an example, consider a counting process that transitions from  $n$  to  $n + 1$  with probability  $\lambda$  at each instant, that is,  $\omega_{n, n+1} = \lambda$  and  $\omega_{nm} = 0$  for  $m \neq n + 1$ . Then the master equation reads

$$\frac{\partial}{\partial t} P(n, t) = \lambda [P(n - 1, t) - P(n, t)] \quad (26.60)$$

(end of example)

This type of equation can be solved through the use of the  $z$ -transform of the sequence  $P(n, t)$ , defined as

$$F(z, t) = \mathcal{Z}[P(n, t)] = \sum_{n=0}^{\infty} z^n P(n, t) \quad (26.61)$$

Then

$$\sum_{n=0}^{\infty} z^n \frac{\partial}{\partial t} P(n, t) = \sum_{n=0}^{\infty} \frac{\partial}{\partial t} (z^n P(n, t)) = \frac{\partial}{\partial t} F(z, t) \quad (26.62)$$

and

$$\sum_{n=0}^{\infty} z^n P(n - 1, t) = z \sum_{n=1}^{\infty} z^{n-1} P(n - 1, t) = z \sum_{n=0}^{\infty} z^n P(n, t) = zF(z, t) \quad (26.63)$$

so that

$$\sum_{n=0}^{\infty} z^n \lambda [P(n - 1, t) - P(n, t)] = \lambda \left[ \sum_{n=0}^{\infty} z^n P(n - 1, t) - \sum_{n=0}^{\infty} z^n P(n, t) \right] = \lambda(z - 1)F(z, t) \quad (26.64)$$

resulting in

$$\frac{\partial}{\partial t} F(z, t) = \lambda(z - 1)F(z, t) \quad (26.65)$$

If  $P(n, 0) = \delta_{n,0}$ , it is easy to check that  $F(z, 0) = 1$ . With this initial condition, (26.65) can be easily integrated yielding

$$F(z, t) = \exp(\lambda(z - 1)t) = \sum_{n=0}^{\infty} z^n \frac{(\lambda t)^n}{n!} e^{-\lambda t} \quad (26.66)$$



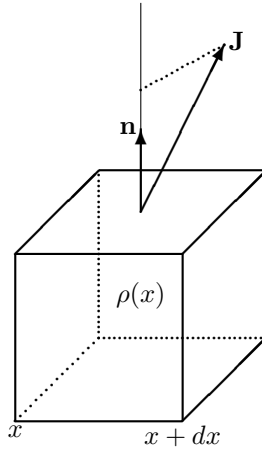


Figure 26.23: Schematic view of the model for the derivation of the diffusion equation;  $\rho(\mathbf{x}, t)$  is the local density of particle,  $\mathbf{J}(\mathbf{x}, t)$  is the population flow: the number of particles that move in a given direction, at a given point and at a given time.

Comparing with (26.61) we have that  $P(n, t)$  follows a Poisson distribution

$$P(n, t) = \frac{(\lambda t)^n}{n!} e^{-\lambda t} \tag{26.67}$$

(end of example)

#### 26.4.4 Macroscopic level--Fokker-Planck equations

##### Diffusion

I shall introduce the macroscopic level of description in a slightly more general setting that needed here before seeing how it related to Brownian motion: as *diffusion*. As I mentioned, the macroscopic level consists in considering that the characteristic magnitudes of the walk (time and distance between collisions) are much smaller than the magnitudes we are considering. This means that we can characterize the problem using a continuous *population density*  $\rho(\mathbf{x}, t)$ : the number of particles in a unit volume around  $\mathbf{x}$  at time  $t$  (Figure 26.23). We can approximate the local density of particles with a continuous field, and take the limit for space and time going to zero. In addition to the density, we define the population flow  $\mathbf{J}(\mathbf{x}, t)$ , which is a vector pointing in the direction of movement and indicating how many particles move per unit time in a surface patch of unitary area. Considering a closed volume  $V$  with a closed surface  $S$ , if there is no generation or annihilation of particles, the variation in density is due to the particles that enter and leave through the surface. So, we have:

$$\frac{\partial}{\partial t} \int_V \rho(\mathbf{x}, t) dV = - \oint_S \mathbf{J}(\mathbf{x}, t) \cdot \mathbf{n} dS \tag{26.68}$$

where  $\mathbf{n}$  is the normal to the surface at  $\mathbf{x}$ . By the divergence theorem:

$$\oint_S \mathbf{J}(\mathbf{x}, t) \cdot \mathbf{n} dS = \int_V \nabla \cdot \mathbf{J} dV \tag{26.69}$$

Applying this theorem to (26.68) we have

$$\int_V \left[ \frac{\partial \rho(\mathbf{x}, t)}{\partial t} + \nabla \cdot \mathbf{J}(\mathbf{x}, t) \right] dV = 0 \quad (26.70)$$

Since the volume  $V$  is arbitrary, we get the continuity equation

$$\frac{\partial \rho(\mathbf{x}, t)}{\partial t} + \nabla \cdot \mathbf{J}(\mathbf{x}, t) = 0 \quad (26.71)$$

In order to get a solvable equation in  $\rho$ , we need to determine how  $\mathbf{J}$  emerges as a consequence of variations of the population density, that is, how  $\mathbf{J}$  relates to  $\rho$ . Such an expression is called a *constitutive equation*. One common constitutive equation, known as *Fick's law*, assume that the flow is proportional to the local population gradient, that is

$$\mathbf{J}(\mathbf{x}, t) = -D \nabla \rho(\mathbf{x}, t) \quad (26.72)$$

The minus sign takes into account the fact that the flow goes from regions of high density to regions of low density. Introducing (26.72) into (26.71) one gets the diffusion equation

$$\frac{\partial \rho}{\partial t} = \nabla \cdot (D \nabla \rho) \quad (26.73)$$

If  $D$  is a constant independent of  $\mathbf{x}$  then (26.73) turns into

$$\frac{\partial \rho}{\partial t} = D \nabla^2 \rho \quad (26.74)$$

and, in the one-dimensional case

$$\frac{\partial \rho}{\partial t} = D \frac{\partial^2 \rho}{\partial x^2} \quad (26.75)$$

This *diffusion equation* has, in principle, nothing to do with Brownian motion or random walks: it has been derived considering a completely different problem, namely the diffusion of a fluid into space under the action of the gradient of its density. Yet, surprisingly, it turns out that this equation does indeed describe Brownian motion. In particular, it describes the evolution of the probability of finding a Brownian walker in  $x$  at time  $t$ .

#### Fokker-Planck equation

The *Fokker-Planck equation* is a partial differential equation in time and space that describes Brownian motion at a macroscopic level. This makes it a macroscopic equation, since the use of differential operators entails that we are considering times and distances much greater than the time and space between changes in direction of a particle. In this section we present the Einstein derivation of the Fokker-Planck equations considering, for the sake of simplicity, the one-dimensional case [15].

The motion of a particle in a Brownian motion can be interpreted as a series of jumps that can have an arbitrary length  $z$ . Let the jump lengths be distributed according to a PDF  $\phi(z)$ , and let them be i.i.d. The density of individuals at position  $x$  at time  $t + \tau$  is given by those individuals that were at a position  $z$  at time  $t$  and that have jumped to  $x$  after waiting a time  $\tau$ . Since  $z$  is arbitrary, we integrate over all possible  $z$ , obtaining a form of non-Markovian Chapman-Kolmogorov equation

$$\rho(x, t + \tau) = \int_{-\infty}^{\infty} \rho(x - z, t) \phi(z) dz \quad (26.76)$$

Note that this equation is continuous in space and discrete in time. In particular, the PDF  $\phi(z)$ , which in ecology is called the *dispersion kernel* is continuous, meaning that we are making an implicit assumption of a large number of individuals/particles. If we now take the macroscopic limit, that is, we consider that  $\tau$  and  $z$  are both small with respect to the scale of interest, then we can use a Taylor expansion in  $t$  and  $z$ :

$$\begin{aligned}\rho(x, t + \tau) &= \sum_{n=0}^{\infty} \frac{\tau^n}{n!} \frac{\partial^n \rho}{\partial \tau^n} \\ \rho(x - z, t) &= \sum_{n=0}^{\infty} \frac{(-z)^n}{n!} \frac{\partial^n \rho}{\partial z^n}\end{aligned}\tag{26.77}$$

Inserting into (26.76), one gets:

$$\rho(x, t) + \tau \frac{\partial \rho}{\partial \tau} + \dots = \rho(x, t) \int_{-\infty}^{\infty} \phi(z) dz - \frac{\partial \rho}{\partial x} \int_{-\infty}^{\infty} z \phi(z) dz + \frac{\partial^2 \rho}{\partial x^2} \int_{-\infty}^{\infty} \frac{z^2}{2!} \phi(z) dz + \dots\tag{26.78}$$

The kernel  $\phi(z)$  is a PDF, therefore  $\int_{-\infty}^{\infty} \phi(z) dz = 1$ . Moreover, if the movements are isotropic, that is, there is no preferential direction of movement, then  $\phi(z) = \phi(-z)$ , and  $\int_{-\infty}^{\infty} z^n \phi(z) dz = 0$  for  $n$  odd. So, we have:

$$\rho(x, t) + \tau \frac{\partial \rho}{\partial \tau} + O(\tau^2) = \rho(x, t) + \frac{\partial^2 \rho}{\partial x^2} \int_{-\infty}^{\infty} \frac{z^2}{2!} \phi(z) dz + O(z^4)\tag{26.79}$$

Or, simplifying the common term and dividing by  $\tau$ ,

$$\frac{\partial \rho}{\partial \tau} = \frac{\partial^2 \rho}{\partial x^2} \int_{-\infty}^{\infty} \frac{z^2}{2\tau} \phi(z) dz + O(z^4/\tau^2)\tag{26.80}$$

We now take the macroscopic limit  $z, \tau \rightarrow 0$ , but in such a way that  $\lim z^2/\tau = C \neq 0$ , that is, keeping  $z^2$  and  $\tau$  of the same order of magnitude. Then we obtain, as a Fokker-Planck equation, a diffusion equation like (26.74):

$$\frac{\partial \rho}{\partial t} = D \frac{\partial^2 \rho}{\partial x^2}\tag{26.81}$$

where

$$D = \frac{1}{2\tau} \int_{-\infty}^{\infty} z^2 \phi(z) dz = \frac{\langle z^2 \rangle}{2\tau}\tag{26.82}$$

Note that (26.81) depends only on the second moment of the diffusion kernel  $\phi(z)$ . In no place have we made the hypothesis that  $\phi(z)$  is Gaussian so very different diffusion kernels with the same second moment will generate the same Fokker-Planck equation. We have lost information with respect to the distribution  $\phi(z)$ : in particular, *given any distribution, a Gaussian distribution with the same second moment will generate the same macroscopic distribution.*

In this sense, we also notice that the Langevin equation does indeed make the hypothesis that  $\xi(t)$  is Gaussian. It would therefore seem that the Einstein derivation is more general than the Langevin equation. In reality, it is not so, and the reason is the Central Limit Theorem<sup>4</sup>: the hypothesis that  $z^2$  and  $\tau$  be of the same magnitude entails that  $D$  is finite and therefore, by (26.81), that  $\langle Z^2 \rangle$  is finite. We are in the hypotheses of the Central Limit Theorem, so the sum of all the jumps of the Einstein's derivation, with distribution  $\phi(z)$ , will end up being Gaussian regardless of the exact shape of  $\phi(z)$ .

<sup>4</sup>We shall not do the derivation here, but from the Langevin equation one can derive the same Fokker-Planck equation as from the Einstein's derivation. So, despite the different hypotheses the two methods describe the same macroscopic phenomenon.

### Solution of the Diffusion Equation

One simple way to solve the diffusion equation is through the use of the Characteristic function of the distribution  $\rho$ , viz. its Fourier Transform. Taking the Fourier transform of (26.75) we get the ordinary differential equation

$$\frac{d\tilde{\rho}}{dt}(\omega, t) = -D\omega^2\tilde{\rho}(\omega, t) \quad (26.83)$$

which has solution

$$\tilde{\rho}(\omega, t) = \tilde{\rho}(\omega, 0) \exp[-D\omega^2 t] \quad (26.84)$$

In the simplest case, at the beginning all the individuals are concentrated at  $x_0$ , that is,  $\rho(x, 0) = \delta(x - x_0)$ . By the formula for the characteristic function of the Dirac distribution (A.44), we have  $\tilde{\rho}(\omega, 0) = \exp[-i\omega x_0]$ . That is

$$\tilde{\rho}(\omega, t) = \exp[-i\omega x_0 - D\omega^2 t] \quad (26.85)$$

The inverse Fourier transform gives us

$$\rho(x, t) = \frac{1}{2\pi} \int_{-\infty}^{\infty} e^{i\omega x} \tilde{\rho}(\omega, t) d\omega = \frac{1}{2\pi} \int_{-\infty}^{\infty} \exp[i\omega(x - x_0) - D\omega^2 t] d\omega = \frac{1}{\sqrt{4\pi Dt}} \exp\left[-\frac{(x - x_0)^2}{4Dt}\right] \quad (26.86)$$

From this solution we can obtain the general solution for  $\rho(x, 0) = g(x)$ . Writing

$$g(y) = \int_{-\infty}^{\infty} g(x) \delta(x - y) dy \quad (26.87)$$

and applying superposition we have

$$\rho(x, t) = \frac{1}{\sqrt{4\pi Dt}} \int_{-\infty}^{\infty} g(y) \exp\left[-\frac{(y - x_0)^2}{4Dt}\right] dy \quad (26.88)$$

With reference to the simple solution (26.86), Figure 26.24 shows  $\rho(x, t)$  as a function of  $x$  for several values of  $t$ . The result is typical of diffusion processes in which the population, initially concentrated at  $x = 0$  ( $\rho(x, 0) = \delta(x)$ ) spreads over larger and larger areas. The "speed" of this diffusion is determined by the increasing variance  $\sigma(t) = \langle X^2 \rangle = 2Dt$  which, as predicted by (A.16) and (26.81), grows linearly with  $t$ .

#### 26.4.5 Anomalous Diffusion

The standard diffusion process, which we have considered so far, is characterized by the relation

$$\langle X^2 \rangle \sim t \quad (26.89)$$

where the notation is shorthand for

$$\lim_{t \rightarrow \infty} \frac{\langle X^2 \rangle}{t} = C \neq 0 \quad (26.90)$$

The reason for this boils down to the fact that the diffusion equation has first derivatives in time and second derivatives in space, so that one obtain homologous quantities starting with a constant and integrating once in time and twice in space.

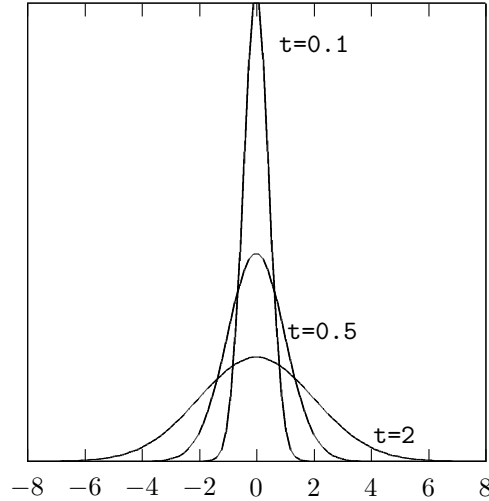


Figure 26.24: The solution of the diffusion  $\rho(x,t)$  for  $\rho(x,0) = \delta(x)$  as a function of  $x$  for several values of  $t$ . The density is a Gaussian that becomes progressively more spread, indicating that the population covers larger and larger areas.

To see a different kind of behavior, consider *ballistic displacements*, that is, the motion of a particle that moves at a constant speed  $v$  and never changes direction. For a movement along the  $x$  axis, this can be modeled as a stochastic process with PDF  $P(x,t) = \delta(x - vt)$  so that

$$\langle X^2 \rangle = \int_{-\infty}^{\infty} x^2 \delta(x - vt) dx = v^2 t^2 \sim t^2 \tag{26.91}$$

That is, in this case

$$\lim_{t \rightarrow \infty} \frac{\langle X^2 \rangle}{t^2} = C \neq 0 \tag{26.92}$$

We can see ballistic movement as a type of random walk, albeit a not-quite-so-random one, and one that moves from the origin much faster than the Brownian motion. Small wonder: ballistic movement moves purposely in a fixed direction, while Brownian motion is bounced to and fro. Note, however, that this means that ballistic movement will explore around much less than Brownian motion: it will stick to a trajectory and not look around at all. Just like a traveler in a rush: you may go very far, but you miss the view.

Processes that don't follow the standard diffusion law (26.89) are called *anomalous* [21]. Ballistic movement is our first example of anomalous diffusion (albeit a rather pathological one). The asymptotic relation between  $\langle X^2 \rangle$  and  $t$  is normally defined using the *Hurst exponent*  $H$  [26] defined by

$$\langle X^2 \rangle \sim t^{2H} \tag{26.93}$$

Diffusion corresponds to  $H = 1/2$ ; if  $H < 1/2$  we have *subdiffusion*, while for  $1/2 < H < 1$  we have *superdiffusion*. The ballistic limit (26.91) is achieved for  $H = 1$  (see Figure 26.25). Note that, because of the central limit theorem, normal diffusion ( $H = 1/2$ ) is obtained under a wide family of displacements distributions. If the displacements:

- i) are independent,
- ii) are identically distributed, and

iii) follow a PDF with finite mean and variance,

then we can apply the CLT in its standard form, and the total distance covered (that is, the sum of all these displacements) is a Gaussian  $\exp(-x^2/\sigma^2)$ , where  $\sigma^2$  is proportional to the number of displacements, that is,  $\sigma^2 \sim t$ . Then (26.89) follow directly from the equality  $\langle X^2 \rangle = \sigma^2$  valid for a Gaussian.

The hypotheses i)--iii) hint at three possible ways in which they can be violated, resulting in three different mechanisms that can generate anomalous diffusion.

- i) the displacements are not independent due to long range correlations: once a particle moves, it will tend to remain in motion (leading to superdiffusion---ballistic motion is an example of this kind of process) or, contrariwise<sup>5</sup>, once it stops it will tend to remain at rest (leading to subdiffusion);
- ii) the distribution of the displacements is not identical, either because they become shorter with time (leading to subdiffusion) or because they become longer (leading to superdiffusion);
- iii) the displacements are distributed according to a PDF with infinite variance, so that arbitrary large displacements are relatively likely.

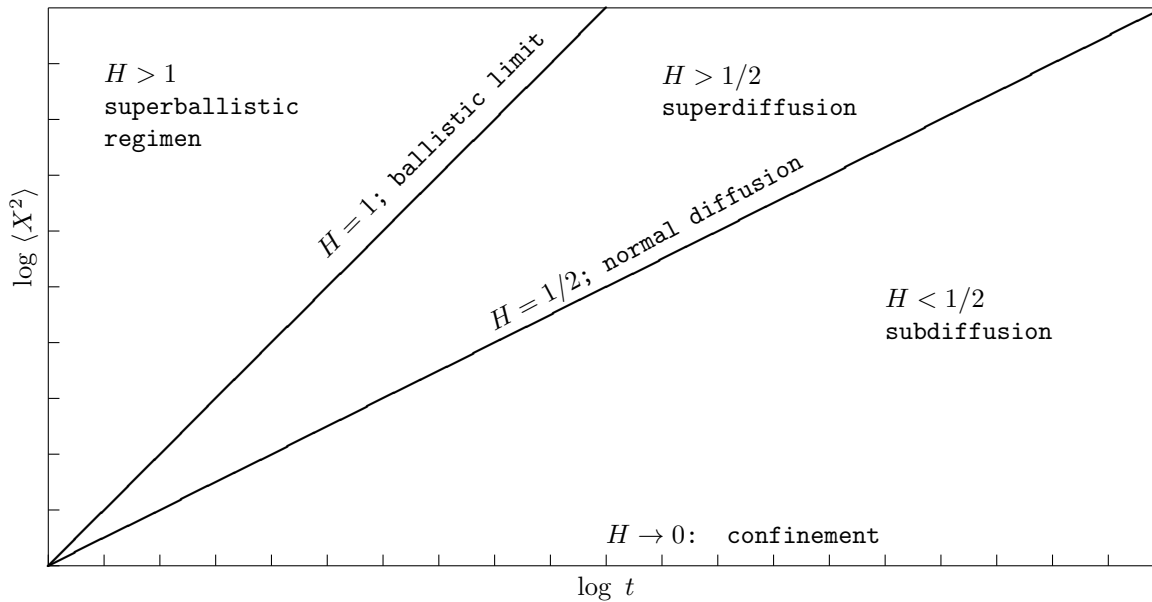


Figure 26.25: The Hurst exponent quantifies the asymptotic behavior of diffusive processes. The usual uncorrelated Brownian random walks satisfy the standard form of the central limit theorem, and have  $H = 1/2$ . Subdiffusive processes have  $H < 1/2$ . For vanishing  $H$ , the process is localized and confined: diffusion has a finite reach. Superdiffusion, viz. processes with a propagation speed higher than Brownian diffusion, have  $H > 1/2$ . The ballistic limit is reached for  $H = 1$ . Superballistic processes (not considered here) correspond to accelerated particles. Lévy flights and walks, of special interest here, are superdiffusive processes.

<sup>5</sup>Neologism courtesy of Lewis Carroll.

In the following, we shall consider mostly the third case but, before digging into it, I shall give a brief example of how the first two work.

**Example IV:**

For the case of long-term correlations, divide the trajectory into intervals of fixed duration  $\Delta t$ . With this division, the correlations between displacements are the same as those between velocities. In this case, we can determine the derivative of  $\langle X^2 \rangle$  as

$$\frac{d}{dt} \langle X^2 \rangle = \frac{d}{dt} \int_0^t \int_0^t \langle v(s)v(\tau) \rangle d\tau ds = 2 \int_0^t \langle v(t)v(\tau) \rangle d\tau \quad (26.94)$$

This result is known as the Taylor's formula [42] (also known as the Green-Kubo formula). If  $\langle v(t)v(\tau) \rangle$  is integrable, then the limit for  $t \rightarrow \infty$  of the integral exists, so the right-hand side of (26.94) is asymptotically a constant, that is, for  $t \rightarrow \infty$ ,

$$\frac{d}{dt} \langle X^2 \rangle \sim C \quad \text{or} \quad \langle X^2 \rangle \sim t \quad (26.95)$$

and we find again a diffusive behavior. If, on the other hand, the correlation decays slowly enough that the integral diverges, then the CLT doesn't hold, and we observe anomalous diffusion. If, for example,  $\langle v(t)v(\tau) \rangle \sim (t - \tau)^{-\eta}$ , with  $0 < \eta < 1$ , then  $\langle X^2 \rangle \sim t^{2-\eta}$ , that is, we have superdiffusion.

(end of example)

**Example V:**

Non-identical displacements occur when displacements become either longer or shorter with time or, equivalently, as the particle gets farther from its initial position. If we take a macroscopic point of view---that is, if we write a diffusion-like Fokker-Planck equation---then we can model this as a time and/or space varying coefficient  $D$ . This is tantamount to saying that the obstacles to motions become gradually larger or smaller as we get away from the initial position. Consider a space-dependent diffusion coefficient that varies as a power law:  $D = D_0 x^\theta$ . This leads to a diffusion equation:

$$\frac{\partial \rho}{\partial t} = \nabla \cdot (D_0 x^\theta \nabla \rho) \quad (26.96)$$

A rigorous derivation of the behavior of  $\langle X^2 \rangle$  under this equation can be found in [32]; here we shall do a simple informal derivation using dimensional analysis. The density  $\rho$  is a number of particles per unit of  $x$  that is, dimensionally,  $[\rho] = [x]^{-1}$  and, consequently

$$\left[ \frac{\partial \rho}{\partial t} \right] = [x]^{-1} [T]^{-1} \quad (26.97)$$

where  $T$  is the dimension of time. Similarly  $[\nabla \rho] = [x]^{-2}$ ,  $[x^\theta \nabla \rho] = [x]^{\theta-2}$  and  $[\nabla \cdot (x^\theta \nabla \rho)] = [x]^{\theta-3}$ . This equality gives us

$$[x]^{-1} [T]^{-1} = \left[ \frac{\partial \rho}{\partial t} \right] = [\nabla \cdot (x^\theta \nabla \rho)] = [x]^{\theta-3} \quad (26.98)$$

that is,  $[T]^{-1} = [x]^{\theta-2}$ ,  $[T] = [x]^{2-\theta}$ , or  $[x] = [T]^{1/(2-\theta)}$ , which leads to

$$[x^2] = [x]^2 = [T]^{\frac{2}{2-\theta}} = [X^2] \quad (26.99)$$

This dimensional equality indicates that, asymptotically,

$$\langle X^2 \rangle \sim t^{\frac{2}{2-\alpha}} \quad (26.100)$$

leading, again, to anomalous diffusion.

(end of example)

The case of divergent moments that I shall consider closely is that of *Lévy flights*. If the individual displacements are i.i.d., then we are in the conditions of the generalized Central Limit Theorem: no matter what the individual PDF are, the sum of a large number of them will converge to a Lévy stable distribution. So, just like in the finite moment case we could assume that the displacements followed a Gaussian distribution<sup>6</sup>, we can now assume that they follow a Lévy distribution which, as seen in (A.41), behaves like  $x^{-(1+\alpha)}$  for  $t \rightarrow \infty$ . For  $\alpha < 2$ ,  $\langle X^2 \rangle$  diverges due to the "long tail" of the distribution, which makes arbitrarily large displacements relatively frequent.

In order to frame these ideas properly, it is first necessary to study random walks from a slightly more general point of view, that of Continuous Time Random Walks.

#### 26.4.6 Continuous Time Random Walks

The random walks that we have considered so far were limits of what we can consider a discrete time scenario: we considered that jumps take place at regular time intervals, and we take the limit of  $\Delta t \rightarrow 0$ , corresponding to a continuum of jumps of length zero (this is enforced by the fact that we require  $\langle x^2 \rangle / \tau$  to stay finite). In a *Continuous Time Random Walk* (CTRW) we assume that the waiting time between jumps is a random process as well, that is, that the particle will intersperse jumps of random length with pauses of random duration. I shall introduce the analysis of CTRW in two steps: first I shall consider the PDF of the position of the particle after  $n$  jumps, without considering *when* did these jumps occur, then the probability of doing  $n$  jumps in time  $t$ . This corresponds to a specific type of CTRW, one in which the jump length is independent of the waiting time. The result can easily be extended to the case in which waiting time and jump length are correlated.

Let  $Z_n$  be the length of the  $n$ th jump. The position of a particle after  $n$  jumps is

$$X_n = \sum_{k=1}^n Z_k = X_{n-1} + Z_n \quad (26.101)$$

This equation shows that the walk is a Markov chain. Let  $Z_k$  be i.i.d. with PDF  $\phi(z)$ ; the function  $\phi$  (the dispersal kernel) represents the transition probability of the Markov chain. Adapting the Chapman-Kolmogorov equation (26.76) to this discrete-time scenario, we obtain an equation for  $\rho_n(x)$ , the density of individuals after  $n$  jumps:

$$\rho_n(x) = \int_{-\infty}^{\infty} \rho_{n-1}(x-z)\phi(z) dz = \rho_{n-1} * \phi \quad (26.102)$$

---

<sup>6</sup>Remember that the Langevin equation, which assume Gaussian displacements, leads to the same macroscopic result as the Einstein method, which doesn't.



where  $*$  denotes spatial convolution. If  $\rho_0$  is the initial density, then:

$$\begin{aligned} \rho_1 &= \rho_0 * \phi \\ \rho_2 &= \rho_1 * \phi = \rho_0 * \phi * \phi \\ &\vdots \\ \rho_n &= \rho_{n-1} * \phi = \rho_0 * \overbrace{\phi * \dots * \phi}^n \end{aligned} \tag{26.103}$$

Considering, for the sake of simplicity, the one-dimensional case, we can take the Fourier transform and apply (A.79) to obtain

$$\tilde{\rho}_n(\omega) = \tilde{\rho}_0(\omega) \tilde{\phi}^n(\omega) \tag{26.104}$$

Consider now the jump times. Let  $\theta_n$  be the waiting time between jump  $n-1$  and jump  $n$ , and  $\psi(t)$  its PDF. The time at which the  $n$ th jump is taken is then

$$T_n = \sum_{k=1}^n \theta_k \tag{26.105}$$

Let  $\psi^0(t)$  be the probability that no jump has occurred by time  $t$ , viz.

$$\psi^0(t) = \int_t^\infty \psi(u) du = 1 - \int_0^t \psi(u) du \tag{26.106}$$

Let  $P_n(t)$  be the probability of performing  $n$  jumps by time  $t$ . Then, clearly,  $P_0(t) = \psi^0(t)$ . The probability that there is a jump at a time  $u < t$  and then no further jumps until time  $t$  is  $\psi(u)\psi^0(t-u)$ . Integrating over all  $u < t$  we have<sup>7</sup>

$$P_1(t) = \int_0^t \psi(u)\psi^0(t-u) du = \psi * \psi \tag{26.107}$$

Iterating this, we have

$$P_n(t) = \psi^0 * \overbrace{\psi * \dots * \psi}^n \tag{26.108}$$

In this case, since we have different limits and a different convolution, one must use the Laplace transform in lieu of the Fourier:

$$\psi(s) = \int_0^\infty e^{-st} \psi(t) dt \tag{26.109}$$

where  $s \in \mathbb{C}$ .<sup>8</sup>

This leads to

$$\tilde{P}_n(s) = \tilde{\psi}^0(s) \tilde{\psi}^n(s) = \frac{1 - \tilde{\psi}(s)}{s} (\tilde{\psi}(s))^n \tag{26.112}$$

---

<sup>7</sup>The asterisk denotes here convolution in time, which has different integration limits than convolution in space, since  $\psi$  and  $\psi^0$  can only take non-negative arguments. Strictly speaking, we should have used a different symbol. However, since it is usually clear what convolution is being used, I have preferred not to complicate the notation using non-standard symbols.

<sup>8</sup>The Laplace transform has similar properties as the Fourier, but is more general. If  $f(t)$  is a function and  $\mathcal{L}[f]$  is its Laplace transform (which I shall also indicate as  $\tilde{f}$ ), then

$$f(t) = \frac{1}{2\pi i} \lim_{T \rightarrow \infty} \int_{\gamma-iT}^{\gamma+iT} \mathcal{L}[f](s) e^{st} ds \tag{26.110}$$

\* \* \*

Consider now the combination of the two processes. The position of an individual at time  $t$  (assume  $x(0) = 0$ ) is

$$x(t) = \sum_{k=0}^{N(t)} z_k \quad (26.113)$$

where  $N(t)$  is the number of jumps taken before time  $t$ , itself a random variable. We are interested in finding an expression for  $\rho(t)$ , the density of individuals at time  $t$ . If by time  $t$   $n$  jumps have been made, then

$$\rho(x, t | N(t) = n) = \rho_n(x) \quad (26.114)$$

The value of  $\rho(x, t)$  is then given by the value of  $\rho_n$  for all possible  $n$ , weighted by their probability:

$$\rho(x, t) = \sum_{n=0}^{\infty} \rho_n(x) P_n(t) \quad (26.115)$$

that is, taking the Fourier and Laplace transforms:

$$\begin{aligned} \tilde{\rho}(\omega, s) &= \sum_{n=0}^{\infty} \tilde{\rho}_n(\omega) \tilde{P}_n(s) \\ &= \tilde{\rho}(\omega, 0) \frac{1 - \tilde{\psi}(s)}{s} \sum_{n=0}^{\infty} [\phi(\omega)\psi(s)]^n \\ &= \tilde{\rho}(\omega, 0) \frac{1 - \tilde{\psi}(s)}{s} \frac{1}{1 - \phi(\omega)\psi(s)} \end{aligned} \quad (26.116)$$

This is known as the *Montroll-Weiß* equation. I made here the assumption that the waiting times and the jump length are independent, hence the product  $\phi(\omega)\psi(s)$ . If they are not, then their joint probability would be expressed by a distribution  $\phi(\omega, s)$ , and (26.116) becomes

$$\tilde{\rho}(\omega, s) = \tilde{\rho}(\omega, 0) \frac{1 - \tilde{\psi}(s)}{s} \frac{1}{1 - \phi(\omega, s)} \quad (26.117)$$

For any distribution  $\phi(\omega)$  and  $\psi(s)$ , (26.116) allows us to determine the evolution of the density of individuals by taking the inverse Fourier/Laplace transform.

Finite moments: diffusion

The generality of the CTRW notwithstanding, if we assume that  $\phi$  and  $\psi$  have finite moment we still revert to the normal diffusive behavior. In order to see this, we first rearrange

where  $\gamma$  is a real number that exceeds the real part of all singularities of  $\mathcal{L}[f]$ . Also:

$$\begin{aligned} \mathcal{L}\left[\int_0^t f(u)g(t-u) du\right] &= \mathcal{L}[f]\mathcal{L}[g] \\ \mathcal{L}\left[\int_0^t f(u) du\right] &= \frac{1}{s}\mathcal{L}[f] \\ \mathcal{L}[e^{at}f(t)] &= \mathcal{L}[f](s-a) \\ \mathcal{L}[1] &= \frac{1}{s} \end{aligned} \quad (26.111)$$

(26.116) in a more useful form. From (26.116), we write

$$s\tilde{\rho}(\omega, s) - \tilde{\rho}(\omega, 0) = \tilde{\rho}(\omega, 0) \left[ \frac{1 - \psi(s)}{1 - \phi(\omega)\psi(s)} - 1 \right] \quad (26.118)$$

Express, from the same equation

$$\tilde{\rho}(\omega, 0) = \frac{s}{1 - \psi(s)} [1 - \phi(\omega)\psi(s)] \tilde{\rho}(\omega, s) \quad (26.119)$$

Replacing in the right-hand side of (26.118) and simplifying we get

$$s\tilde{\rho}(\omega, s) - \tilde{\rho}(\omega, 0) \frac{s\psi(s)}{1 - \psi(s)} [1 - \phi(\omega)\psi(s)] \tilde{\rho}(\omega, s) \quad (26.120)$$

The quantity

$$M(s) = \frac{s\psi(s)}{1 - \psi(s)} \quad (26.121)$$

is called the *memory kernel* of the CTRW. Equation (26.120) can in turn be rewritten in a way that separates the spatial and temporal variables:

$$\frac{1 - \psi(s)}{s\psi(s)} [s\tilde{\rho}(\omega, s) - \tilde{\rho}(\omega, 0)] = [1 - \phi(\omega)\psi(s)] \tilde{\rho}(\omega, s) \quad (26.122)$$

We now consider the macroscopic limit in space, which entails assuming that the microscopic scale of the process is very small compared to the scale of  $x$ . This means that we shall consider the limit for  $\omega \rightarrow 0$  in the Fourier space. Similarly, the macroscopic limit in time consists in taking the limit  $s \rightarrow 0$  in the complex plane of the Laplace transform. If  $\phi$  is symmetric and has finite moments, then it has an expansion  $\phi(\omega) = 1 - \langle \phi^2 \rangle \omega^2 / 2 + o(\omega^4)$ , where  $\langle \phi \rangle$  is the average displacement  $\langle X^2 \rangle$  when  $X$  has PDF  $\phi$ . Similarly,  $\psi(s) = 1 - \langle \psi \rangle s + o(s^2)$ , where  $\langle \psi \rangle$  is the mean waiting time. From this we get

$$\frac{1 - \psi^0(s)}{s\psi(s)} \sim \frac{\langle \psi \rangle}{1 - \langle \psi \rangle s} = \langle \psi \rangle + o(s) \quad (26.123)$$

while

$$[\phi(\omega) - 1] = -\frac{\langle \phi^2 \rangle}{2} \omega^2 + o(\omega^2) \quad (26.124)$$

Putting these in (26.122) we have

$$\langle \psi \rangle [s\rho(\omega, s) - \rho(\omega, 0)] = \frac{\langle \phi^2 \rangle}{2} \omega^2 \rho(\omega, s) \quad (26.125)$$

that is, taking the inverse Fourier and Laplace transforms

$$\frac{\partial}{\partial t} \rho(x, t) = \frac{\langle \phi^2 \rangle}{2 \langle \psi \rangle} \frac{\partial^2}{\partial x^2} \rho(x, t) \quad (26.126)$$

that is, we are back to a diffusion equation that behaves like (26.93), with  $H = 1/2$ .

We obtain anomalous diffusion in two ways: we can either make long pauses (viz. pauses with a distribution with diverging variance) or we can make long jumps.

## Long pauses

Let us assume that  $\phi(z)$  has a Gaussian distribution<sup>9</sup>, while  $\psi(t)$  has a Lévy distribution with a long tail

$$\psi(t) \sim A_\alpha \left(\frac{\tau}{t}\right)^\alpha \quad (26.127)$$

with  $0 < \alpha < 1$ . We are interested in the long term behavior of the walk, that is, in terms of characteristic functions, in the limit  $\omega \rightarrow 0$ ,  $|s| \rightarrow 0$  so we can write

$$\begin{aligned} \phi(\omega) &= \exp\left(-\frac{\omega^2 \sigma^2}{2}\right) \sim 1 - \sigma^2 \omega^2 \\ \psi(s) &= \exp(-\tau^\alpha |s|^\alpha) \sim 1 - (\tau s)^\alpha \end{aligned} \quad (26.128)$$

Introducing into (26.116), we get

$$\rho(\tilde{\omega}, s) = \frac{1}{s} \frac{\rho(\omega, 0)}{1 + K_\alpha \omega^2 s^{-\alpha}} \quad (26.129)$$

with  $K_\alpha = \sigma^2 / \tau^\alpha$ . The long term behavior of  $\langle X^2 \rangle$  can be determined using the relation

$$\langle X^2 \rangle = \lim_{\omega \rightarrow 0} -\frac{\partial \tilde{\rho}}{\partial \omega} \quad (26.130)$$

For  $\rho(x, 0) = \delta(x)$ , i.e.  $\tilde{\rho}(\omega, 0) = 1$ , we have

$$\begin{aligned} \langle X^2 \rangle &= \lim_{\omega \rightarrow 0} \left[ -\frac{2}{s} K_\alpha s^{-\alpha} (1 + K_\alpha \omega^2 s^{-\alpha})^{-2} - \frac{8}{s} (1 + K_\alpha \omega^2 s^{-\alpha})^{-3} (K_\alpha s^{-\alpha} \omega^2)^2 \right] \\ &= 2K_\alpha s^{-(\alpha+1)} \end{aligned} \quad (26.131)$$

which, inverting the Laplace transform, gives

$$\langle X^2 \rangle = \frac{2K_\alpha}{\Gamma(\alpha+1)} t^\alpha \quad (26.132)$$

Since  $\alpha < 1$ , we are in the presence of subdiffusion ( $H = \alpha/2 < 1/2$ ), as could be expected given that we have arbitrarily long pauses with relative high frequency.

## Long jumps

We consider now the opposite situation: assume that  $\psi(t)$  has a distribution with finite moments (exponential, in this case, since  $t > 0$ ) and that  $\phi(z)$  has a Lévy distribution with Lévy parameter  $\mu$ :

$$\begin{aligned} \psi(t) &= \tau \exp\left(-\frac{t}{\tau}\right) \\ \phi(z) &= A_\mu \left(\frac{z_0}{z}\right)^{1+\mu} \end{aligned} \quad (26.133)$$

Note that in this case we consider  $1 < \mu < 2$  for the sake of simplicity: the results are similar for  $0 < \mu < 1$ . As before, in the limit  $\omega \rightarrow 0$ ,  $|s| \rightarrow 0$ , we can approximate them as

$$\begin{aligned} \psi(s) &\sim 1 - s\tau \\ \phi(\omega) &\sim 1 - \sigma^\mu \omega^\mu \end{aligned} \quad (26.134)$$

---

<sup>9</sup>As we have seen, any distribution, as long as it has finite moments, will give the same results, as we are in the hypotheses of the standard Central Limit Theorem.

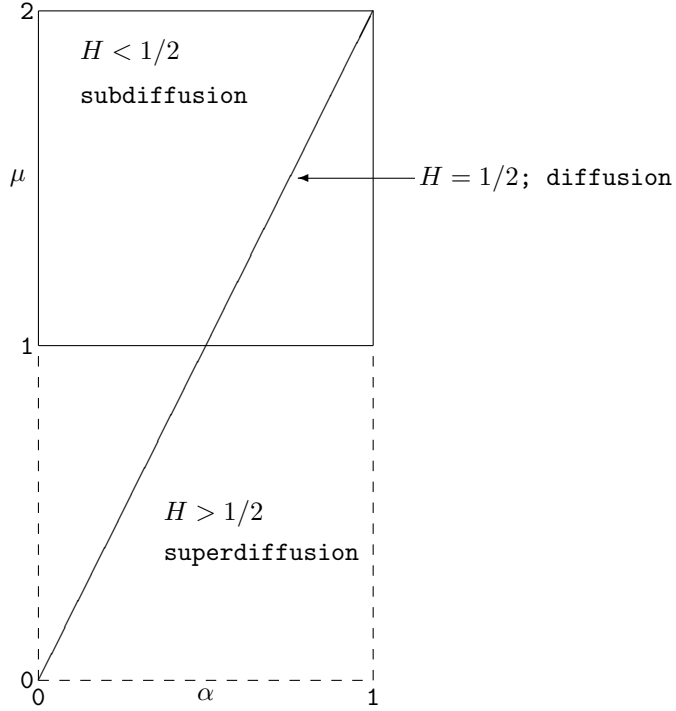


Figure 26.26: Subdiffusion and superdiffusion for long waits and long jumps as a function of the parameters  $\alpha$  and  $\mu$  of the relation  $\langle X^2 \rangle \sim t^{2\alpha/\mu}$ , that is,  $H = \alpha/\mu$  (see text).

Inserting these approximations into (26.116) we have

$$\tilde{\rho}(\omega, s) = \tau \frac{\tilde{\rho}(\omega, 0)}{s + K^\mu \omega^\mu} \tag{26.135}$$

where  $K^\mu = \sigma^\mu/\tau$  or, for  $\rho(x, 0) = \delta(x)$ ,

$$\tilde{\rho}(\omega, s) = \frac{\tau}{s + K^\mu \omega^\mu} \tag{26.136}$$

Taking the inverse Laplace transform, we have

$$\tilde{\rho}(\omega, t) = \exp(-K^\mu \omega^\mu) \tag{26.137}$$

that is, we obtain a Lévy stable distribution, as expected from the generalized Central Limit Theorem. Note that in this case  $\langle X^2 \rangle \rightarrow \infty$ , so we can't directly compare this distribution with the standard diffusion. There are however several ways to arrive at a result. The first is to use a truncated Lévy distribution, which is closer to real applications as in the physical world one doesn't have arbitrarily long jumps. The second is to extrapolate from fractional moments  $\langle X^q \rangle$  with  $q < \mu$ , which can be shown to converge and, in this case:

$$\langle X^q \rangle \sim t^{q/\mu} \tag{26.138}$$

which leads to a Hurst exponent  $H = 1/\mu > 1/2$ , that is, to superdiffusion<sup>10</sup>.

<sup>10</sup>An informal way to reach the same conclusion is to note that  $K^\mu = \sigma^\mu/\tau$  so that, in order to have  $K^\mu$  finite, we must have  $\sigma^\mu \sim \tau$ , that is,  $\sigma^2 \sim \tau^{2/\mu}$ , leading again to  $H = 1/\mu$ .

## Long waits and long jumps

The case in which both jumps and waiting times have Lévy distribution can be treated similarly, leading to

$$\tilde{\rho}(\omega, s) = \frac{1}{s} \frac{1}{1 + K_{\alpha}^{\mu} \omega^{\mu} s^{-\alpha}} \quad (26.139)$$

By analogy with the previous cases, we see that

$$\langle X^2 \rangle \sim t^{2\alpha/\mu} \quad (26.140)$$

which entails  $H = \alpha/\mu$ . If  $\mu > 2\alpha$ , then  $H < 1/2$ , and we have subdiffusion, if  $\mu < 2\alpha$  we have superdiffusion (see figure 26.26).

# Bibliography

- [1] M. J. Acerbo, P. A. Gargiulo, I. Krug, and J. D. Delius. Behavioural consequences of nucleus accumbens dopaminergic stimulation and glutamatergic blocking in pigeons. *Behavioral Brain Research*, 136:171--7, 2002.
- [2] R.J. Bainton, L.T.Y. Tsai, C.M. Singh, M.S. Moore, W.S. Neckameyer, and U. Heberlein. Dopamine modulates response to cocaine, nicotine, and ethanol in *Drosophila*. *Current Biology*, 10:187--94, 2000.
- [3] S.L. Barrett, R. Bell, D. Watson, and D.J. King. Effects of amisulpride, risperidone and chlorpromazine on auditory and visual latent inhibition, prepulse inhibition, executive function and eye movements in healthy volunteers. *Journal of Psychopharmacology*, 18:156--72, 2004.
- [4] G.S. Berns, S.M. McClure, G. Pagnoni, and P.R. Montague. Predictability modulates human brain response to reward. *Journal of Neuroscience*, 21:2793--8, 2001.
- [5] M Bertolucci-D'Angiò, A. Serrano, and B. Scatton. Differential effects of forced locomotion, tail-pinch, immobilization, and methyl-carboline carboxylate on extracellular 3,4-dihydroxyphenylacetic acid levels in the rat striatum, nucleus accumbens, and prefrontal cortex: an in vivo voltammetric study. *Journal of Neurochemistry*, 55:1208--15, 1990.
- [6] T.S. Braver and J.D. Cohen. On the control of control: the role of dopamine in regulating prefrontal function and working memory. In S. Monsell and J. Driver, editors, *Control of Cognitive Processes*, pages 713--37. Cambridge, MA:MIT Press, 2000.
- [7] H. Buxbaum-Conradi and J.P. Ewert. Responses of single neurons in the toad's caudal ventral striatum to moving visual stimuli and test of their different projection by extracellular antidromic stimulation/recording techniques. *Brain, Behavior, and Evolution*, 54:338--54, 1999.
- [8] E. L. Charnov. Optimal foraging: the marginal value theorem. *Theoretical Population Biology*, 9:129--36, 1976.
- [9] T. A. Cleland and A. I. Silverston. Dopaminergic modulation of inhibitory glutamate receptors in the lobster stomatogastric ganglion. *Journal of Neurophysiology*, 78:3450--2, 1997.
- [10] KJ.A. Dani and F. Zhou. Selective dopamine filter of glutamate striatal afferents. *Neuron*, 42:522--3, 2004.

- [11] M.R. DeLong. Primate models of movement disorders of basal ganglia origin. *Trends in Neuroscience*, 13:281--5, 1990.
- [12] M.R. Due, J. Jing, and R.W. Kludiusz. Dopaminergic contributions to modulatory functions of a dual-transmitter interneuron in *Aplysia*. *Neuroscience letters*, 358:53--7, 2004.
- [13] S.M. Dursun, N. Wright, and M.A. Reveley. Effects of amphetamine on saccadic eye movements in man: Possible relevance to schizophrenia? *Journal of Psychopharmacology*, 13:245--7, 1999.
- [14] H. Eichenbaum and N.J. Cohen. *From conditioning to conscious recollection: Memory systems of the brain*. New York:Oxford University Press, 2001.
- [15] Albert Einstein. "uber die von der molekularkinetischen theorie der wärme geforderte bewegung von in ruhenden flüssigkeiten suspendierten teilchen. *Annalen der Physics*, 17:549--560, 1905.
- [16] J.L. Evenden, M. Turpin, L. Oliver, and C. Jennings. Caffeine and nicotine improve visual tracking by rats: a comparison with amphetamine, cocaine and apomorphine. *Psychopharmacology (Berlin)*, 110:169--76, 1993.
- [17] S.B. Floresco, D.N. Braaksma, and A.G. Phillips. Involvement of the ventral pallidum in working memory tasks with or without a delay. *Annals of the New York Academy of Sciences*, 877:711--6, 1999.
- [18] S.B. Floresco, J.K. Seamans, and A.G. Phillips. A selective role for dopamine in the nucleus accumbens of the rat in random foraging but not delayed spatial win-shift-based foraging. *Behavioral Brain Research*, 80:161--8, 1996.
- [19] Crispin W Gardiner. *Stochastic methods*. Springer-Verlag, Berlin--Heidelberg--New York--Tokyo, 1985.
- [20] R.M. Harris-Warrick, L.M. Coniglio, N. Barazangi, J. Guckenheimer, and S. Gueron. Dopamine modulation of transient potassium current evokes phase shifts in a central pattern generator network. *Journal of Neuroscience*, 15:342--58, 1995.
- [21] S. Havlin and D. Benavraham. Diffusion in disordered media. *Advances in Physics*, 36:695--798, 1987.
- [22] Takeyuki Hida. Brownian motion. In *Brownian Motion*, pages 44--113. Springer, 1980.
- [23] T. Hills, P. J. Brockie, and A. V. Maricq. Dopamine and glutamate control area-restricted search behavior in *Caenorhabditis elegans*. *Journal of Neuroscience*, 24:1217--25, 2004.
- [24] Thomas T. Hills. Animal foraging and the evolution of goal-directed cognition. *Cognitive Science*, 30:3--41, 2006.
- [25] C.S. Holling. Some characteristics of simple types of predation and parasitism. *Canadian Entomology*, 91:385--98, 1959.
- [26] H.E. Hurst, R.P. Black, and Y.M. Simaika. *Long-term storage: an experimental study*. London:Constable, 1965.



- [27] Ioannis Karatzas and Steven Shreve. *Brownian motion and stochastic calculus*, volume 113. Springer Science & Business Media, 2012.
- [28] Vicenç Méndez, Daniel Campos, and Frederic Bartumeus. *Stochastic foundations in movement ecology*. Springer Series in Synergetics. Berlin:Springer-Verlag, 2014.
- [29] Melanie Mitchell. *An introduction to genetic algorithms*. Cambridge, MA:MIT press, 1998.
- [30] D.R. Nassel. Neuropeptides, amines and amino acids in an elementary insect ganglion: Functional chemical anatomy of the unfused abdominal ganglion. *Progress in Neurobiology*, 48:325--420, 1996.
- [31] P. O'Donnel and A. Grace. Synaptic interactions among excitatory afferents to nucleus accumbens neurons: Hippocampal gating of prefrontal cortical input. *Journal of Neuroscience*, 15:3622--39, 1995.
- [32] B O'Shaughnessy and I. Procaccia. Analytical solutions for diffusion on fractal objects. *Physical Review Letters*, 54(5):455--8, 1985.
- [33] J. G. Powles. Brownian motion--june 1827. *Physics Education*, 13:310--2, 1978.
- [34] William H. Press, Brian P. Flannery, Saul A. Teulolsky, and William T. Vetterling. *Numerical Recipes, The Art of Scientific Computing*. Cambridge University Press, 1986.
- [35] A. Reiner. Catecholaminergic innervation of the basal ganglia in mammals: Anatomy and function. In A.J. Smeets and A. Reiner, editors, *Phylogeny and development of catechoamine systems in the CNS of vertebrates*. Cambridge, England:Cambridge University Press, 1994.
- [36] A. Reiner, L. Medina, and C.L. Veenman. Structural and functional evolution of the basal ganglia in vertebrates. *Brain Research Reviews*, 28:235--85, 1998.
- [37] C. Salas, C. Broglio, and F. Rodriguez. Evolution of firebrain and spatial cognition in vertebrates: Conservation across diversity. *Brain, Behavior and Evolution*, 62:72--82, 2003.
- [38] W. Schultz. Neural coding of basic reward terms of animal learning theory, game theory, microeconomics and behavioural ecology. *Current Opinions in Neurobiology*, 14:139--44, 2004.
- [39] W. Schultz, R. Romo, T. Ljungberg, J. Mirenowicz, J.R. Hoolerman, and A. Dickinson. Reward-related signals carried by dopamine neurons. In J.C. Houk, J.L. Davis, and D.G. Beiser, editors, *Models of information processing in the basal ganglia*, pages 233--48. Cambridge, MA:MIT Press, 1995.
- [40] J.K. Seamans, S.B. Floresco, and A.G. Phillips. D1 receptor modulation of hippocampal-prefrontal cortical circuits integrating spatial memory with executive functions in the rat. *Journal of Neuroscience*, 18:1613--21, 1998.
- [41] D. W. Stephens. *Foraging Theory*. Princeton:Princeton University Press, 1986.
- [42] G.I. Taylor. Diffusion by continuous movements. *Proceedings of the London Mathematical Society* 2, 20:196--212, 1921.

- [43] S.P. Tipper, B. Weaver, L.M. Jerreat, and A.L. Burak. Object-based and environment-based inhibition of return of visual attention. *Journal of Experimental Psychology: Human Perception and Performance*, 20:478--99, 1994.
- [44] M. Wang, S. Vijayraghavan, and P.S. Goldman-Rakic. Selective D2 receptor actions on the functional circuit of working memory. *Science*, 303:853--6, 2004.
- [45] J.G. White, E. Southgate, J.N. Thomson, and S. Brenner. The structure of the nervous system in the neumatode *Caenorhabditis Elegans*. *Philosophical Transactions of the Royal Society of London B; Biological Sciences*, 314:1--340, 1986.

# Appendix A

## A.1 RANDOM VARIABLES

A *random variable* is a mathematical object characterized by a set  $\Omega$  (the *range* of the variable), which contains all possible outcomes of the variable and a function  $P_X(x)$ <sup>1</sup> that assigns, to each  $x \in \Omega$  a value  $P_X(x) \in [0,1]$  called its *probability*. The function  $P_X$  is not arbitrary, but must meet some minimal conditions. If the set  $\Omega$  is finite or countable, these conditions can be expressed simply as

i)  $\forall x \in \Omega. P_X(x) \geq 0$  (positivity)

ii)  $\sum_{x \in \Omega} P_X(x) = 1$  (normalization)

If  $\Omega$  is uncountable, the conditions are technically more complex. In this case,  $X$  is a continuous random variable, and  $P_X$  is referred to as the *probability density function* (PDF) of  $X$ . The function  $P_X$  in this case represents a probability only if it is integrated over a subset of  $\Omega$  of non-zero measure. In this case, the normalization condition is

$$\int_{\Omega} P_X(x) dx = 1 \tag{A.1}$$

If  $\Omega = \mathbb{R}$  (as we shall often assume) we have

$$\int_{-\infty}^{\infty} P_X(x) dx = 1 \tag{A.2}$$

For continuous variables on  $\mathbb{R}$  one can define the *cumulative probability function*, that is, the probability that  $X$  be at most  $x$ :

$$\mathcal{P}(x) = \mathbb{P}[X \leq x] = \int_{-\infty}^x P_X(u) du \tag{A.3}$$

Note that

$$P_X(x) = \frac{\partial}{\partial x} \mathcal{P}(x). \tag{A.4}$$

From this and the positivity condition we can derive that  $\mathcal{P}$  is monotonically non-decreasing and that

$$\lim_{x \rightarrow -\infty} \mathcal{P}(x) = 0 \quad \lim_{x \rightarrow \infty} \mathcal{P}(x) = 1 \tag{A.5}$$

---

<sup>1</sup>Following the standard notation, we shall use capital letters to indicate random variables and lowercase letters to indicate the values that they assume.

In some cases, a whole function might be difficult to work with; it is easier to work with an enumerable set of numbers that characterizes the function completely. *Statistical moments* are such quantities. The moment of order  $n$  of the variable  $X$  is defined as

$$\langle X^n \rangle = \int_{\Omega} x^n P_X(x) dx \quad (\text{A.6})$$

In general, given a function  $f$  defined on  $\Omega$ , we define

$$\langle f(X) \rangle = \int_{\Omega} f(x) P_X(x) dx \quad (\text{A.7})$$

The  $n$ th moment is obtained for  $f(x) = x^n$ .

The first order moment  $\langle X \rangle$  is called the *mean*, the *average*, or the *expected value* of  $X$ , while

$$\sigma^2 = \langle X^2 \rangle - \langle X \rangle^2 \quad (\text{A.8})$$

is the *variance*; its square root  $\sigma$  is the *standard deviation* of  $X$ .

Not all distributions have finite moments, that is, the integral (A.6) may fail to converge. If the moments are finite, then they completely characterize the PDF. To show this, we introduce the *characteristic function*  $\tilde{P}_X(\omega)$  of a PDF  $P_X$ :

$$\tilde{P}_X(\omega) = \langle e^{i\omega x} \rangle = \int_{\Omega} e^{i\omega x} P_X(x) dx \quad (\text{A.9})$$

This is simply the Fourier transform of  $P_X$ , so the PDF can be recovered from its characteristic function as

$$P_X(x) = \frac{1}{2\pi} \int e^{-i\omega x} \tilde{P}_X(\omega) d\omega \quad (\text{A.10})$$

The relation with the moments becomes evident by taking the Taylor expansion of the exponential:

$$e^{i\omega x} = \sum_n \frac{(i\omega x)^n}{n!} \quad (\text{A.11})$$

Introducing this into (A.9) we get

$$\tilde{P}_X(\omega) = \sum_n \frac{(i\omega)^n}{n!} \int x^n P_X(x) dx = \sum_n \frac{(i\omega)^n}{n!} \langle X^n \rangle \quad (\text{A.12})$$

As a consequence, the moments of  $P_X$  can be obtained by differentiating  $\tilde{P}_X$ :

$$\langle X^n \rangle = \lim_{\omega \rightarrow 0} (-i)^n \frac{\partial^n}{\partial \omega^n} \tilde{P}_X(\omega) \quad (\text{A.13})$$

\* \* \*

The *joint probability* of two random variables  $X_1$  and  $X_2$ , indicated as  $P_{X_1 \cap X_2}(x_1, x_2)$  measures the simultaneous probability that  $X_1$  and  $X_2$  take the values  $x_1$  and  $x_2$ , respectively. The *conditional probability*  $P_{X_1|X_2}(x_1|x_2)$  denotes the probability that  $X_1$  take value  $x_1$  conditioned to the fact that  $X_2$  takes value  $x_2$ . Two variables are *independent* if for all  $x_1, x_2$   $P_{X_1|X_2}(x_1|x_2) = P_{X_1}(x_1)$ , that is, knowing the value of  $X_2$  does not change the distribution of  $X_1$ . Joint and conditional probabilities are related through Bayes's theorem:

$$P_{X_1 \cap X_2}(x_1, x_2) = P_{X_1|X_2}(x_1|x_2)P_{X_2}(x_2) = P_{X_2|X_1}(x_2|x_1)P_{X_1}(x_1) \quad (\text{A.14})$$

### A.1.1 Useful Probability Distributions

A variable  $X$  follows a **Gaussian** (or *normal*) distribution if

$$P_X(x) = \frac{1}{\sigma\sqrt{2\pi}} \exp\left(-\frac{(x-\mu)^2}{\sigma^2}\right) \tag{A.15}$$

(Figure A.1) or, equivalently, it has characteristic function

$$\tilde{P}_X(\omega) = \int_{-\infty}^{\infty} e^{i\omega x} P_X(x) dx = \exp\left(i\omega\mu - \frac{\omega^2\sigma^2}{2}\right) \tag{A.16}$$

The mean of the distribution is  $\langle X \rangle = \mu$ . Note that, for  $\mu = 0$ , the characteristic function has

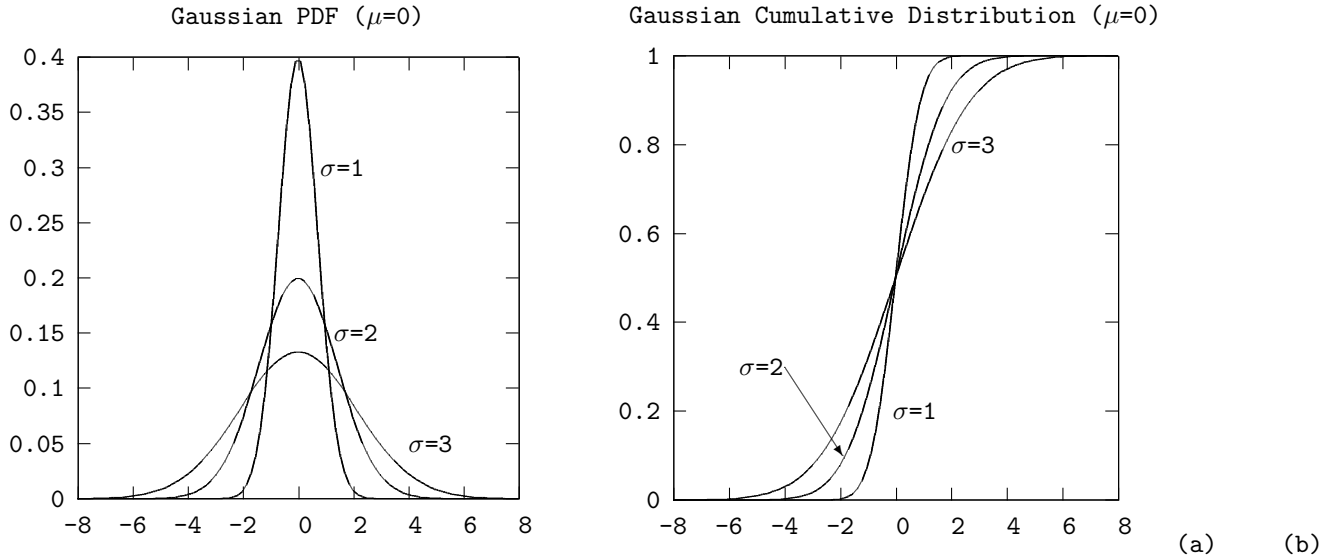


Figure A.1: The Gaussian PDF (a) and the corresponding cumulative distribution (b) for various values of  $\sigma$ ; in all cases it is  $\mu = 0$ .

also the functional form of a Gaussian, a fact that will have important consequences. In this special case ( $\mu = 0$ ) the moments are given by

$$\langle X^n \rangle = \int_{-\infty}^{\infty} x^n \frac{1}{\sigma\sqrt{2\pi}} \exp\left(-\frac{(x-\mu)^2}{\sigma^2}\right) dx = \begin{cases} \frac{2^{\frac{n}{2}} \sigma^n}{\sqrt{\pi}} \Gamma\left(\frac{n+1}{2}\right) & n \text{ even} \\ 0 & n \text{ odd} \end{cases} \tag{A.17}$$

where  $\Gamma$  is Euler's Gamma function. An important moment is

$$\langle X^2 \rangle = \sigma^2 + \langle X \rangle. \tag{A.18}$$

One important property of the Gaussian distribution, vis-à-vis the Central Limit Theorem (which we shall consider in the following), is that it is *stable*: if  $X, Y$  are Gaussians, and  $a, b \in \mathbb{R}$ , then  $aX + bY$  is also Gaussian.

Let  $X$  and  $Y$  be two Gaussian-distributed variables with zero mean and variance  $\sigma_1^2$  and  $\sigma_2^2$ , respectively. Then

$$\begin{aligned}\tilde{P}_X(\omega) &= \exp\left(-\frac{\omega^2\sigma_1^2}{2}\right) \\ \tilde{P}_Y(\omega) &= \exp\left(-\frac{\omega^2\sigma_2^2}{2}\right)\end{aligned}\tag{A.19}$$

and consequently

$$\tilde{P}_X(\omega)\tilde{P}_Y(\omega) = \exp\left(-\frac{\omega^2(\sigma_1^2 + \sigma_2^2)}{2}\right)\tag{A.20}$$

that is, the product of the characteristic function of two Gaussian distributions is still the characteristic function of a Gaussian distribution.

\* \* \*

The Gaussian distribution is defined for all  $x \in \mathbb{R}$ , but many variables that one might be interested in modeling assume only positive values in such a way that the probability that  $x = 0$  is 0 and, after reaching a maximum, decreases rapidly for high values of  $x$ . The most different things can be observed to have this distribution, from the length of messages in internet fori to the prices of hotels, or the size of particles in a collision.

All these phenomena can be modeled as following a **logonormal distribution**. A variable  $X$  has logonormal distribution if  $\log X$  has normal (viz. Gaussian) distribution. Let  $\Phi$  and  $\phi$  be the cumulative distribution and the density of a normally distributed variable with 0 mean and unit variance ( $\mathcal{N}(0,1)$ ), and assume  $\log X \sim \mathcal{N}(\mu, \sigma)$ , i.e.  $\log X$  has a normal distribution with mean  $\mu$  and variance  $\sigma^2$ . Then

$$\begin{aligned}P_X(x) &= \frac{d}{dx}\mathcal{P}_X(x) = \frac{d}{dx}\mathbb{P}[X \leq x] \\ &= \frac{d}{dx}\mathbb{P}[\log X \leq \log x] \\ &= \frac{d}{dx}\Phi\left[\frac{\log x - \mu}{\sigma}\right] \\ &= \phi\left[\frac{\log x - \mu}{\sigma}\right] \frac{d}{dx}\left[\frac{\log x - \mu}{\sigma}\right] \\ &= \frac{1}{\sigma x} \phi\left[\frac{\log x - \mu}{\sigma}\right] \\ &= \frac{1}{\sqrt{2\pi}\sigma x} \exp\left[-\frac{(\log X - \mu)^2}{2\sigma^2}\right]\end{aligned}\tag{A.21}$$

Figure A.2 shows the behavior of the logonormal PDF for various values of  $\sigma$  and  $\mu = 0$ . Note that  $\mu$  and  $\sigma$  are the mean and variance of  $\log X$ , not of  $X$ . To distinguish them, I shall indicate the mean and the variance of  $X$  as  $m$  and  $v$ , respectively.

The moments of  $X$  are given by

$$\langle X^n \rangle = \int_0^\infty x^n P_X(x) dx = \exp\left(n\mu + \frac{n^2\sigma^2}{2}\right)\tag{A.22}$$

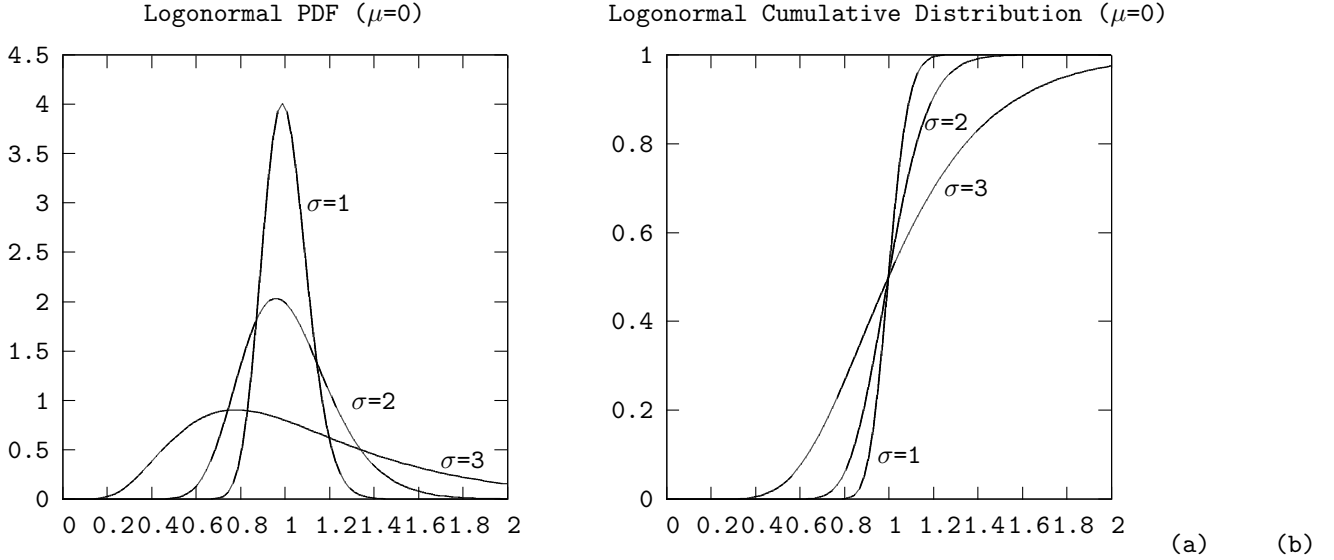


Figure A.2: The logonormal PDF (a) and the corresponding cumulative distribution (b) for various values of  $\sigma$ ; in all cases it is  $\mu = 0$ .

as can be verified by replacing  $z = \frac{1}{\sigma} [\log X - (\mu + n\sigma^2)]$  in the integral. From this we have

$$\begin{aligned}
 m &= \langle X \rangle = \exp\left(\mu + \frac{\sigma^2}{2}\right) \\
 \langle X^2 \rangle &= \exp(2\mu + 2\sigma^2) \\
 v &= \langle X^2 \rangle - \langle X \rangle^2 = \exp(2\mu + \sigma^2)(e^{\sigma^2} - 1)
 \end{aligned}
 \tag{A.23}$$

From these equality, one can derive the values of  $\mu$  and  $\sigma^2$  for desired  $m$  and  $v$ :

$$\mu = \log \frac{m}{\sqrt{1 + \frac{v}{m^2}}} \quad \sigma^2 = \log \left(1 + \frac{v}{m^2}\right)
 \tag{A.24}$$

The characteristic function  $\langle \exp(i\omega x) \rangle$  is defined, but if we try to extend it to complex variables,  $\langle \exp(sx) \rangle$ ,  $s \in \mathbb{C}$  is not defined for any  $s$  with a negative imaginary part. This entails that the characteristic function is not analytical in the origin and, consequently, it can't be represented as an infinite convergent series. In particular, the formal Taylor series

$$\sum_n \frac{(i\omega x)^n}{n!} \langle x^n \rangle = \sum_n \frac{(i\omega x)^n}{n!} \exp\left(n\mu + \frac{n^2\sigma^2}{2}\right)
 \tag{A.25}$$

diverges

\* \* \*

Other positive variables follow a different distribution, one in which the value 0 is the most probable, and the probability decreases sharply as  $x$  increases, In these cases, the variable  $x$

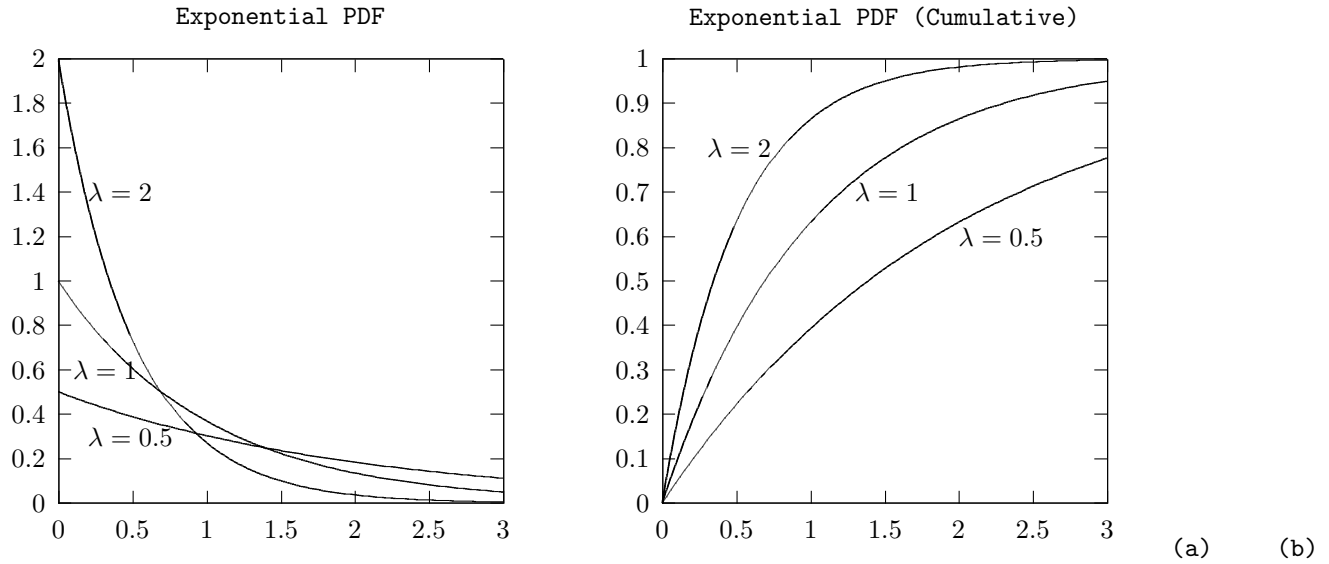


Figure A.3: The exponential PDF (a), and the corresponding cumulative distribution in (b) for various values of  $\lambda$ .

can be modeled using an **exponential** distribution:

$$P_X(x) = \begin{cases} \lambda e^{-\lambda x} & x \geq 0 \\ 0 & x < 0 \end{cases} \tag{A.26}$$

If the variable can take negative values, then

$$P_X(x) = \frac{\lambda}{2} e^{-\lambda|x|} \tag{A.27}$$

(Figure A.3. Its characteristic function is

$$\tilde{P}_X(\omega) = \frac{\lambda^2}{\lambda^2 + \omega^2} \tag{A.28}$$

and its moments

$$\langle X^n \rangle = \frac{1}{\lambda^n} \Gamma(n + 1) \tag{A.29}$$

\* \* \*

A **uniform** or *flat* distribution assigns the same probability density to each point in  $\Omega$ . So, if  $\Omega = [a, b]$ ,

$$P_X(x) = \begin{cases} \frac{1}{b-a} & a \leq x \leq b \\ 0 & \text{otherwise} \end{cases} \tag{A.30}$$

The characteristic function of the uniform distribution is

$$\tilde{P}_X(\omega) = \frac{e^{i\omega b} - e^{i\omega a}}{i\omega(b - a)} \tag{A.31}$$



and its moments

$$\langle X^n \rangle = \frac{1}{n+1} \frac{b^{n+1} - a^{n+1}}{b-a} \tag{A.32}$$

\* \* \*

A **Cauchy**, or **Lorentz** distribution has PDF

$$P_X(x) = \frac{1}{\pi} \frac{\gamma}{x^2 + \gamma^2} \tag{A.33}$$

where  $\gamma$  is a positive parameter, and characteristic function

$$\tilde{P}_X(\omega) = e^{-\gamma|\omega|} \tag{A.34}$$

If one tries to compute the moments using the definition

$$\langle X^n \rangle = \frac{\gamma}{\pi} \int \frac{x^n}{x^2 + \gamma^2} dx \tag{A.35}$$

then, since the integrand behaves as  $x^{n-2}$  for  $x \rightarrow \infty$ , one observes that they diverge for  $n \geq 1$ . This limits the usefulness of this distribution as a model of real phenomena (which typically have finite moments), and in practice one "truncates" the distribution to a finite interval  $[a, b]$ .

\* \* \*

We have mentioned that one important property of the Gaussian distribution is the preservation of the functional form of their characteristic function under multiplication, as in (A.20). The Gaussian distribution is not the most general distribution with this property (although it is the only one with this property *and* finite moments): it is shared by the family of **Lévy distributions**. Lévy distributions depend on four parameters:  $\alpha$  (Lévy index),  $\beta$  (skew),  $\mu$  (shift), and  $\sigma$  (scale), and they are defined through their characteristic function:

$$\tilde{P}_{\alpha,\beta}(\omega; \mu, \sigma) = \int_{-\infty}^{\infty} e^{i\omega x} P_{\alpha,\beta}(x; \mu, \sigma) dx \triangleq \exp \left[ i\mu\omega - \sigma^\alpha |\omega|^\alpha \left( 1 - i\beta \frac{\omega}{|\omega|} \Phi \right) \right] \tag{A.36}$$

where

$$\Phi = \begin{cases} \tan \frac{\alpha\pi}{2} & \alpha \neq 1, 0 < \alpha < 2 \\ -\frac{2}{\pi} \ln |x| & \alpha = 1 \end{cases} \tag{A.37}$$

the four parameters determine the shape of the distribution. Of these,  $\alpha$  and  $\beta$  play a major rôle in this note, while  $\mu$  and  $\sigma$  can be eliminated through proper scale and shift transformations (much like mean and variance for the Gaussian distribution):

$$P_{\alpha,\beta}(x; \mu, \sigma) = \frac{1}{\sigma} P_{\alpha,\beta}\left(\frac{x-\mu}{\sigma}; 0, 1\right) \tag{A.38}$$

From now on, I shall therefore ignore  $\mu$  and  $\sigma$  and refer to the distribution as  $P_{\alpha,\beta}(x)$ . Note the symmetry relation

$$P_{\alpha,-\beta}(x) = P_{\alpha,\beta}(x) \tag{A.39}$$

The distributions with  $\beta = 0$  are symmetric, and these are the ones that are the most relevant in this context. The closed form of  $P_{\alpha,\beta}$  is known only for a few cases. If  $\alpha = 2$  one obtains the Gaussian distribution ( $\beta$  is irrelevant, since  $\Phi = 0$ ); if  $\alpha = 1, \beta = 0$  one obtains the Cauchy distribution, and for  $\alpha = 1/2, \beta = 1$ , the Lévy-Smirnov distribution

$$P_{1/2,1}(x) = \begin{cases} \frac{1}{\sqrt{2\pi}} x^{-3/2} \exp(-\frac{1}{2x}) & x \geq 0 \\ 0 & x < 0 \end{cases} \quad (\text{A.40})$$

The most important property in this context is the asymptotic behavior of  $P_{\alpha,\beta}$  which is given by the power law

$$P_{\alpha,0}(x) \sim \frac{C(\alpha)}{|x|^{1+\alpha}} \quad (\text{A.41})$$

with

$$C(\alpha) = \frac{1}{\pi} \sin\left(\frac{\pi\alpha}{2}\right) \Gamma(1+\alpha) \quad (\text{A.42})$$

This power law behavior entails that arbitrarily large values are relatively probable (compared with the exponential decay of the Gaussian). Consequently, as can be expected,  $\langle X^2 \rangle$  diverges for  $\alpha < 2$ .

\* \* \*

The **Dirac delta distribution** is a pathological distribution useful in many contexts; for example, when dealing with certainty in a probabilistic framework, or when analyzing discrete random variables in a context created for continuous ones. The distribution is:

$$P_X(x) = \delta(x - x_0) \quad (\text{A.43})$$

where  $\delta(\cdot)$  is the Dirac distribution. The characteristic function of the distribution is

$$\tilde{P}_X(\omega) = \exp(i\omega x_0). \quad (\text{A.44})$$

The function  $\delta(x)$  is zero everywhere except for  $x = 0$ , and

$$\int_{-\infty}^{\infty} \delta(x) dx = 1 \quad (\text{A.45})$$

This property entails  $\delta(ax) = \delta(x)/a$ . Also

$$\int_{-\infty}^{\infty} f(x) \delta(x - x_0) dx = f(x_0) \quad (\text{A.46})$$

from which we derive

$$\langle x^n \rangle = x_0^n \quad (\text{A.47})$$

\* \* \*

Unlike the previous distribution, the **binomial distribution** is defined for discrete variables, in particular for a variable  $X$  that can take two values, the first one with probability  $p$ , and the second one with probability  $1-p$ . Suppose, for example, that we play a game in which, at each turn, I have a probability  $p$  of winning and  $1-p$  of losing (think of head-and-tails game with a tricked coin). If we play  $N$  rounds of the game, what is the probability that I win exactly  $n$  times? This turns out to be

$$P(X = n) = \binom{N}{n} p^n (1-p)^{N-n} = \frac{N!}{n!(N-n)!} p^n (1-p)^{N-n} \tag{A.48}$$

which is precisely the binomial distribution. Its characteristic function is

$$\tilde{P}(\omega) = (1-p + pe^{i\omega})^N \tag{A.49}$$

from which the moments can be derived. For example

$$\langle X \rangle = \lim_{\omega \rightarrow 0} \frac{d\tilde{P}}{d\omega} = \lim_{\omega \rightarrow 0} pN e^{i\omega} (1-p + pe^{i\omega})^{N-1} = pN \tag{A.50}$$

\* \* \*

An important and common distribution, one that appears as a limiting case of many finite processes, is the **Poisson Distribution**. Its importance will probably be more evident if we derive it as a limiting case in some examples.

**Example VI:**

Consider events that may happen at any moment in time (the events are punctual: they have no duration). Divide the time-line in small intervals of duration  $\Delta t$ , so short that the probability that two or more events will take place in the same interval is negligible. Assume that the probability that one event take place in  $[t, t + \Delta t)$  is constant, and proportional to the length of the interval:

$$P(1; \Delta t) = \lambda \Delta t \tag{A.51}$$

and, because no two events happen in the same interval,

$$P(0; \Delta t) = 1 - \lambda \Delta t \tag{A.52}$$

Let  $P(0; t)$  be the probability that no event has taken place up to time  $t$ . Then

$$P(0; t + \Delta t) = P(0; t)(1 - \lambda \Delta t) \tag{A.53}$$

Rearranging the terms we get

$$\frac{P(0; t + \Delta t) - P(0; t)}{\Delta t} = -\lambda P(0; t) \tag{A.54}$$

and, taking the limit for  $\Delta t \rightarrow 0$

$$\frac{\partial}{\partial t} P(0; t) = -\lambda P(0; t) \tag{A.55}$$

that is,  $P(0; t) = C \exp(-\lambda t)$  or, considering the boundary condition  $P(0, 0) = 1$ ,

$$P(0; t) = e^{-\lambda t} \tag{A.56}$$

This takes care of the case in which no event takes place before time  $t$ . On to the general case. There were  $n$  events by time  $t + \Delta t$  if either (1) we had  $n$  events up to time  $t$  and no event occurred in  $[t, t + \Delta t]$ , or (2) there were  $n - 1$  events at  $t$  and one event occurred in  $[t, t + \Delta t]$ . This leads to

$$P(n; t + \Delta t) = (1 - \lambda \Delta t)P(n; t) + \lambda \Delta t P(n - 1; t) \quad (\text{A.57})$$

rearranging and taking the limit  $\Delta t \rightarrow 0$ , we have

$$\frac{\partial}{\partial t} P(n; t) + \lambda P(n; t) = \lambda P(n - 1; t) \quad (\text{A.58})$$

In order to transform this equation into a more manageable form, we look for a function that, multiplied by the left-hand side, transforms it into the derivative of a product. That is, we look for a function  $\mu(t)$  such that

$$\mu(t) \left[ \frac{\partial P}{\partial t} + \lambda P \right] = \frac{\partial}{\partial t} [\mu(t) P] \quad (\text{A.59})$$

It is easy to verify that  $\mu(t) = \exp(\lambda t)$  fits the bill. Equation (A.58) therefore becomes

$$\frac{\partial}{\partial t} [e^{\lambda t} P(n; t)] = e^{\lambda t} \lambda P(n - 1; t) \quad (\text{A.60})$$

For  $n = 1$  we have

$$\frac{\partial}{\partial t} [e^{\lambda t} P(1; t)] = e^{\lambda t} \lambda e^{-\lambda t} = \lambda \quad (\text{A.61})$$

That is, integrating both sides and multiplying by  $e^{-\lambda t}$

$$P(1; t) = \lambda t e^{-\lambda t} \quad (\text{A.62})$$

For arbitrary  $n$ , I'll show by induction that

$$P(n; t) = \frac{(\lambda t)^n}{n!} e^{-\lambda t} \quad (\text{A.63})$$

We have already derived the result for  $n = 0$  and for  $n = 1$ . For arbitrary  $n$ , we have

$$\begin{aligned} \frac{\partial}{\partial t} [e^{\lambda t} P(n + 1; t)] &= e^{\lambda t} \lambda P(n; t) \\ &= e^{\lambda t} \lambda \frac{(\lambda t)^n}{n!} e^{-\lambda t} \quad (\text{induction hypothesis}) \\ &= \lambda \frac{(\lambda t)^n}{n!} \end{aligned} \quad (\text{A.64})$$

So, integrating

$$e^{\lambda t} P(n + 1; t) = \frac{\lambda}{n!} \int (\lambda t^n) dt = \frac{(\lambda t)^{n+1}}{(n + 1)!} + C \quad (\text{A.65})$$

where  $C = 0$  because of the initial conditions, so

$$P(n + 1; t) = e^{-\lambda t} \frac{(\lambda t)^{n+1}}{(n + 1)!} \quad (\text{A.66})$$

(end of example)

The distribution that results from this example:

$$P_X(x) = e^{-x} \frac{x^n}{n!} \quad (\text{A.67})$$

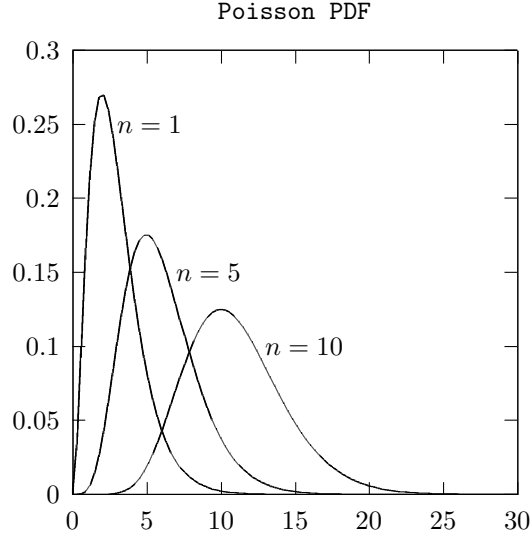


Figure A.4: The Poisson PDF for various values of  $n$ .

is the Poisson distribution that, in the example, gives us the probability that  $n$  events take place in a time  $x$ . Figure A.4 shows the shape of this distribution as a function of  $x$  for various values of  $n$ .

**Example VII:**

The Poisson distribution can also be seen as a limiting case of the binomial distribution. If  $p$  is the probability of success, then  $\nu = Np$  is the expected number of successful trials, as per (A.50). This approximation is valid for large  $N$ . In this case, we have

$$P(n; N) = \frac{N!}{n!(N-n)!} \left(\frac{\nu}{N}\right)^n \left(1 - \frac{\nu}{N}\right)^{N-n} \quad (\text{A.68})$$

Taking  $N \rightarrow \infty$ , we have

$$\begin{aligned} P_\nu(n) &= \lim_{N \rightarrow \infty} P(n; N) \\ &= \lim_{N \rightarrow \infty} \frac{N \cdot (N-1) \cdots (N-n+1)}{n} \frac{\nu^n}{N^n} \left(1 - \frac{\nu}{N}\right)^N \left(1 - \frac{\nu}{N}\right)^{-n} \\ &= \lim_{N \rightarrow \infty} \frac{N \cdot (N-1) \cdots (N-n+1)}{N^n} \frac{\nu^n}{n!} \left(1 - \frac{\nu}{N}\right)^N \left(1 - \frac{\nu}{N}\right)^{-n} \\ &= 1 \cdot \frac{\nu^n}{n!} e^{-\nu} \cdot 1 \\ &= \frac{\nu^n}{n!} e^{-\nu} \end{aligned} \quad (\text{A.69})$$

So, once again, we find that the number of successes has a Poisson distribution.

(end of example)

The characteristic function of the distribution (A.67) is

$$\tilde{P}(\omega) = e^{\lambda(e^{i\omega} - 1)} \quad (\text{A.70})$$

from which we obtain

$$\langle X \rangle = \lambda \quad (\text{A.71})$$

### A.1.2 Functions of Random Variables

If  $X$  is a random variable on  $\Omega$ , and  $f: \Omega \rightarrow \Omega'$ , then  $Y = f(X)$  is a random variable on  $\Omega'$ . Here I'll consider, for the sake of simplicity, the case  $\Omega = \Omega' = \mathbb{R}$  (all our considerations can be generalized to arbitrary continua  $\Omega$  under fairly general conditions, essentially that  $\Omega$  be a metric space). In order to determine the distribution of  $y$ , I begin with a preliminary observation. For a random variable  $X$ , let  $\mathbb{P}_X[x, x + \Delta x]$  the probability that the value of  $X$  falls in  $[x, x + \Delta x]$ . Then, for small  $\Delta x$ ,

$$\begin{aligned} \mathbb{P}_X[x, x + \Delta x] &= P(X \leq x + \Delta x) - P(X \leq x) \\ &= \frac{\partial}{\partial x} P(X \leq x) \Delta x + O(\Delta x^2) \\ &= P_X(x) \Delta x + O(\Delta x^2) \end{aligned} \quad (\text{A.72})$$

Let now  $f$  be invertible, and  $g = f^{-1}$ . Then

$$\begin{aligned} P_Y \Delta y &= \mathbb{P}_Y[y, y + \Delta y] \\ &= \mathbb{P}_X[g(y), g(y + \Delta y)] \\ &\approx \mathbb{P}_X \left[ g(y), g(y) + \left| \frac{dg}{dy} \right| \Delta y \right] \\ &= P_X(g(y)) \left| \frac{dg}{dy} \right| \Delta y \end{aligned} \quad (\text{A.73})$$

from which we get

$$P_Y(y) = P_X(g(y)) \left| \frac{dg}{dy} \right| \quad (\text{A.74})$$

Note that equivalently one could have defined

$$P_Y(y) = \int \delta(y - f(x)) P_X dx = \langle \delta(y - f(x)) \rangle_X \quad (\text{A.75})$$

where the subscript on the average reminds us that we are taking the average with respect to the distribution of  $X$ . From this, we can determine the characteristic function of  $Y$ :

$$\begin{aligned} \tilde{P}_Y(\omega) &= \int e^{i\omega y} P_Y(y) dy \\ &= \int P_X(x) \left[ \int e^{i\omega y} \delta(y - f(x)) dy \right] dx \\ &= \int e^{i\omega f(x)} P_X(x) dx \\ &= \langle \exp[i\omega f(x)] \rangle_X \end{aligned} \quad (\text{A.76})$$

If  $Y = aX$ , then

$$\tilde{P}_Y(\omega) = \langle \exp[i\omega aX] \rangle_X = \tilde{P}_X(a\omega) \quad (\text{A.77})$$

\* \* \*

Consider now the sum of two random variables:  $Z = X + Y$ . Each value of  $Z$  can be obtained through an infinity of events: each time  $X$  takes an arbitrary value  $x$ , and  $y$  takes a value  $z - x$ ,  $Z$  takes the same value, namely  $z$ . Summing up all these possible events we obtain

$$P_Z(z) = \int_{-\infty}^{\infty} P_X(x)P_Y(z - x) dx \tag{A.78}$$

This is known as the *convolution* of  $P_X$  and  $P_Y$ , often indicated as  $P_Z = P_X * P_Y$ . The properties of the Fourier transform entail that the corresponding relation between characteristic functions is

$$\tilde{P}_Z(\omega) = \tilde{P}_X(\omega)\tilde{P}_Y(\omega) \tag{A.79}$$

\* \* \*

Let  $Y = \{y_1, \dots, y_n\}$  be a set of independent and identically distributed (i.i.d.) variables with cumulative distribution  $\mathcal{P}_Y$  and density  $P_Y$ . Consider the function  $\min(Y)$ : we are interested in finding its density  $P_{\min}$  and cumulative distribution  $\mathcal{P}_{\min}$ . We have:

$$\mathcal{P}_Y(x) = \mathbb{P}[\min(Y) \leq x] = 1 - \mathbb{P}[\min(Y) \geq x] \tag{A.80}$$

We have  $\min(Y) \geq x$  iff we have  $y_i \geq x$  for all  $i$ , that is

$$\begin{aligned} \mathcal{P}_{\min}(x) &= 1 - \mathbb{P}[\forall y \in Y. y \geq x] \\ &= 1 - \mathbb{P}[y \geq x]^n \\ &= 1 - \left(1 - \mathbb{P}[y \leq x]\right)^n \\ &= 1 - \left(1 - \mathcal{P}_Y(x)\right)^n \end{aligned} \tag{A.81}$$

The density is

$$\begin{aligned} P_{\min}(x) &= \frac{d}{dx} \mathcal{P}_{\min}(x) \\ &= n \left(1 - \mathcal{P}_Y(x)\right)^{n-1} \frac{d}{dx} \mathcal{P}_Y(x) \\ &= n \left(1 - \mathcal{P}_Y(x)\right)^{n-1} P_Y(x) \end{aligned} \tag{A.82}$$

For the function  $\max(Y)$ , working in a similar way, we have

$$\mathcal{P}_{\max}(x) = (\mathcal{P}_Y(x))^n P_{\max}(x) = n(\mathcal{P}_Y(x))^{n-1} P_Y(x) \tag{A.83}$$

### A.1.3 The Central Limit Theorem

The Central Limit Theorem (important enough to be granted its own acronym: CLT) is one of the fundamental results in basic probability theory and the main reason why the Gaussian distribution is so important and so common in modeling natural events. In a nutshell, the

theorem tells us the following: if we take a lot of random variables, independent and identically distributed (i.i.d.), and add them up, the result will be a random variable with Gaussian distribution. So, for example, if we repeat an experiment many times and take the average of the results that we obtain (the average is, normalization apart, a sum), no matter what the characteristics of the experiment are, the resulting average will have (more or less) a Gaussian distribution.

But, ay, there's the rub! The theorem works only in the assumption that the moments of the distributions involved be finite. We shall see shortly what happens if this assumption is not satisfied.

Let  $X_1, \dots, X_n$  be a set of i.i.d. random variables with distribution  $P_X$ , zero mean, and (finite) variance  $\sigma^2$ . Note that  $Y = \sum_i X_i$  has zero mean and variance  $n\sigma^2$ , while  $Y = (\sum_i X_i)/n$  has zero mean and variance  $\sigma^2/n$ . It is therefore convenient to work with the variable

$$Z_n = \frac{1}{\sqrt{n}} \sum_i X_i \quad (\text{A.84})$$

which has zero mean and variance  $\sigma^2$  independently of  $n$ .

*Theorem A.1.1. For any distribution  $P_X$  with finite mean and variance, and  $X_1, \dots, X_n$  i.i.d. with distribution  $P_X$ , for  $n \rightarrow \infty$ , we have  $Z_n \rightarrow Z_\infty$ , where  $Z_\infty$  is a Gaussian random variable with zero mean and variance  $\sigma^2$  equal to the variance of  $P_X$ .*

*Proof.* Consider the first terms of the expansion of the characteristic function of  $P_X$ :

$$\tilde{P}_X(\omega) = \int e^{i\omega x} P_X(x) dx = 1 - \frac{1}{2}\sigma^2\omega^2 + O(\omega^3) \quad (\text{A.85})$$

The characteristic function of  $Y = \sum_i X_i$  is given by (A.79):

$$\tilde{P}_Y(\omega) = \prod_i \tilde{P}_{X_i}(\omega) = [\tilde{P}_X(\omega)]^n \quad (\text{A.86})$$

(the second equality holds because the  $X$ s have the same distribution) while (A.77) with  $a = 1/\sqrt{n}$  gives

$$\tilde{P}_Z(\omega) = P_Y\left(\frac{\omega}{\sqrt{n}}\right) = \left[P_X\left(\frac{\omega}{\sqrt{n}}\right)\right]^n \approx \left(1 - \frac{\sigma^2\omega^2}{2n}\right)^n \xrightarrow{n \rightarrow \infty} \exp\left(-\frac{1}{2}\sigma^2\omega^2\right) \quad (\text{A.87})$$

Finally, from (A.16) we have the inverse transform

$$P_Z(z) = \frac{1}{\sigma\sqrt{2\pi}} \exp\left(-\frac{z^2}{2\sigma^2}\right) \quad (\text{A.88})$$

□

This theorem is true, in the form in which we have presented it, only for distributions  $X$  with finite mean and variance<sup>2</sup>. However, the key to the theorem is an invariance property of the characteristic function of the Gaussian. Consider the equality (A.86); we can split it up as:

$$\tilde{P}_Z(\omega; n) = [\tilde{P}_X(\omega)]^n = [\tilde{P}_X(\omega)]^{n/2} [\tilde{P}_X(\omega)]^{n/2} = \tilde{P}_Z(\omega; n/2) \tilde{P}_Z(\omega; n/2) \quad (\text{A.89})$$

<sup>2</sup>I have assumed zero mean since, if the mean of the  $X$  is non-zero, the mean of  $Z$  goes to infinity; this doesn't represent a major hurdle for the theorem, which can easily be generalized by subtracting the mean from the variables  $X$  and then adding it back.



Taking the limit  $n \rightarrow \infty$ , this gives us  $P_Z(\omega) = P_Z(\omega)P_Z(\omega)$ . That is: the condition for a distribution to be a central limit is that the product of two characteristic functions have the same functional form as the original distributions. As we have seen in (A.20), the Gaussian distribution does have this property. Nay: it is the *only* distribution with finite moments that has this property, hence its appearance in the theorem in the finite moments case, and hence its great importance in application as a model of many processes resulting from the sum of identical sub-processes.

If we abandon the finite moment hypothesis, however, there is a more general distribution to which (A.89) applies: the stable Levy distribution. So, a more general form of the CLT can be enunciated as:

Theorem A.1.2. *For any distribution  $P_X$ , and  $X_1, \dots, X_n$  i.i.d. with distribution  $P_X$ , for  $n \rightarrow \infty$ , we have*

$$\lim_{n \rightarrow \infty} \frac{1}{\sqrt{n}} \sum_{i=1}^n X_i = Z_\infty \tag{A.90}$$

where  $Z_\infty$  is a random variable with Levy distribution. If the variance of  $P_X$  is finite and equal to  $\sigma^2$ , then  $Z_\infty$  has a Gaussian distribution with variance  $\sigma^2$ .

#### A.1.4 Stochastic Processes

A *stochastic process* is a set of random variables  $X(t)$  indexed by a variable  $t$  (commonly identified with time) that takes value either in  $\mathbb{N}$  or  $\mathbb{R}^+$  (less frequently in  $\mathbb{R}$ ). We indicate with  $P(x, t)$  the probability that the process take value  $x$  at time  $t$  (the probability density if  $t$  is continuous; I shall omit the subscript  $X$  to avoid complicating the notation), and with  $P(x_2, t_2; x_1, t_1)$  the joint probability density for the two variables  $X(t_1)$  and  $X(t_2)$ . The multiple joint probability density  $P(x_1, t_1; \dots, x_n, t_n)$  is defined analogously. In the following, whenever possible, I shall use the joint probability  $P(x_2, t_2; x_1, t_1)$  to simplify the notation, but all considerations hold for the more general multiple joint probability.

Just as a stochastic variable is instantiated to a specific value  $x \in \Omega$  with a certain probability, so a stochastic process is instantiated as a trajectory  $X: \mathbb{R} \rightarrow \Omega$  (or with a discrete series  $X: \mathbb{N} \rightarrow \Omega$  if the process is discrete). Each  $X(t)$ , for fixed  $t$ , is a stochastic variable with a probability distribution that, in general, depends on  $t$ . A stochastic process is *stationary* if all these distributions are the same, that is,  $P(x, t) \equiv P(x)$ , or, equivalently, if

$$P(x_1, t_1; x_2, t_2) = P(x_1, t_1 + \tau; x_2, t_2 + \tau) \tag{A.91}$$

In a stochastic process, there are two ways of computing averages: one can compute the *ensemble average*  $\langle X(t) \rangle$ , that is, the average of the random variable  $X(t)$ , or the mean value along a trajectory

$$\bar{X} = \lim_{T \rightarrow \infty} \frac{1}{T} \int_0^T x(t) dt \tag{A.92}$$

A process is *ergodic* if the two coincide

$$\langle X \rangle = \bar{X} \tag{A.93}$$

Ergodicity is an important property for random walks: many times we are interested in the characteristics of the motion of one individual, but many of the equations that we shall use

involve ensemble probabilities based on a whole population. Ergodicity allows us to switch from one to the other with impunity.

Note that in a stationary process the correlation  $\langle X(t_1)X(t_2) \rangle$  does not depend on  $t_1$  and  $t_2$  individually, but only on their difference  $\tau = t_2 - t_1$ . Joint probabilities are positive, symmetric ( $P(x_1, t_1; x_2, t_2) = P(x_2, t_2; x_1, t_1)$ ) and normalized:

$$\iint_{\Omega^2} P(x_1, t_1; x_2, t_2) dx_1 dx_2 = 1 \quad (\text{A.94})$$

Joint probabilities can be reduced by integration

$$P(x_1, t_1) = \int_{\Omega} P(x_1, t_1; x_2, t_2) dx_2 \quad (\text{A.95})$$

and Bayes theorem can be extended to stochastic processes

$$P(x_1, t_2) = \int_{\Omega} P(x_2, t_2 | x_1, t_1) P(x_1, t_1) dx_1 \quad (\text{A.96})$$

A process is Markov if, for all  $t_1 < t_2 < \dots < t_n$ ,

$$P(x_n, t_n | x_{n-1}, t_{n-1}; \dots; x_1, t_1) = P(x_n, t_n | x_{n-1}, t_{n-1}) \quad (\text{A.97})$$

this entails that, at any time, the status of the process encodes all the information necessary to make predictions about its future: it is not necessary to know how the process reached that status. The Markov property can be chained:

$$\begin{aligned} P(x_1, t_1; x_2, t_2; x_3, t_3) &= P(x_2, t_2; x_3, t_3 | x_1, t_1) P(x_1, t_1) \\ &= P(x_3, t_3 | x_2, t_2) P(x_2, t_2 | x_1, t_1) P(x_1, t_1) \end{aligned} \quad (\text{A.98})$$

Finally, it can be shown [19] that Markov processes must satisfy the *Chapman-Kolmogorov* equation:

$$P(x_3, t_3 | x_1, t_1) = \int_{\Omega} P(x_3, t_3 | x_2, t_2) P(x_2, t_2 | x_1, t_1) dx_2 \quad (\text{A.99})$$

The characteristics of the Markov process is evidenced by the fact that the probability of the transition  $(x_1, t_1) \rightarrow (x_2, t_2) \rightarrow (x_3, t_3)$  is the product of the probabilities of the transitions  $(x_1, t_1) \rightarrow (x_2, t_2)$  and  $(x_2, t_2) \rightarrow (x_3, t_3)$ , that is, the two transitions are *statistically independent*.

### A.1.5 Gaussian and Wiener processes

I shall provide here some details on two types of processes of considerable importance for random walks and diffusion.

A stochastic process  $X(t)$  is Gaussian with zero mean if  $\langle X(t) \rangle = 0$  and

$$P(x_i, t_i) = \sqrt{\frac{A_{ii}}{2\pi}} \exp\left(-\frac{1}{2} A_{ii} x_i^2\right) \quad (\text{A.100})$$

( $A_{ii} > 0$ ). The joint probability  $P(x_1, t_1; \dots; x_n, t_n)$  then follows a multivariate Gaussian distribution

$$P(x_1, t_1; \dots; x_n, t_n) = \frac{\det(\mathbf{A})^{1/2}}{(2\pi)^{n/2}} \exp\left[-\frac{1}{2} \sum_{i,j=1}^n x_i A_{ij} x_j\right] \quad (\text{A.101})$$

Where  $\mathbf{A} \in \mathbb{R}^{n \times n}$  is symmetric (strictly) positive definite. The matrix  $\mathbf{A}$  is a measure of the covariance between two variables of the Gaussian process

$$\langle X(t_i)X(t_j) \rangle = (\mathbf{A}^{-1})_{ij} \quad (\text{A.102})$$

(this is true since we assume zero mean). A process is uncorrelated if  $\langle X(t_i)X(t_j) \rangle = D\delta(t_i - t_j)$ , in which case  $A_{ij} = D^{-1}\delta_{ij}$ .

A *Wiener process*  $W$  is a process in which the variables  $W(t)$  are real and with independent increments  $W(t_2) - W(t_1)$  that follow a Gaussian distribution. That is, they define a conditional probability

$$P(w_2, t_2 | w_1, t_1) = \frac{1}{\sigma\sqrt{2\pi(t_2 - t_1)}} \exp\left[-\frac{(w_2 - w_1)^2}{2\sigma^2(t_2 - t_1)}\right] \quad (\text{A.103})$$

from which the covariance can be computed

$$\begin{aligned} \langle (W(t_2) - \langle W \rangle)(W(t_1) - \langle W \rangle) \rangle &= \langle (W(t_2) - W(0))(W(t_1) - W(0)) \rangle \\ &= \int_{-\infty}^{\infty} (w_2 - w_0) dw_2 \int_{-\infty}^{\infty} dw_1 (w_1 - w_0) P(w_2, t_2; w_1, t_1) \\ &= \sigma^2 \min(t_1, t_2) + w_0^2 \end{aligned} \quad (\text{A.104})$$

From this we get

$$\langle W(t)^2 \rangle = \sigma^2 t + w_0^2 \quad (\text{A.105})$$

Wiener processes are related to Gaussian processes, in particular to uncorrelated (white) Gaussian processes. Let  $X(t)$  be a Gaussian process with  $\langle X(t_1)X(t_2) \rangle = \sigma^2\delta(t_2 - t_1)$ , and define a new stochastic process as the integral of  $X(t)$ :

$$Y(t) = \int_0^t X(u) du \quad (\text{A.106})$$

then

$$\begin{aligned} \langle Y(t_2)Y(t_1) \rangle &= \int_0^{t_2} du_2 \int_0^{t_1} du_1 \langle X(u_1)X(u_2) \rangle \\ &= \int_0^{t_2} du_2 \int_0^{t_1} du_1 \delta(u_2 - u_1) \end{aligned} \quad (\text{A.107})$$

By the properties of the Dirac function

$$\int_0^{t_1} du_1 \delta(u_2 - u_1) = \begin{cases} 1 & 0 < u_2 < t_1 \\ 0 & \text{otherwise} \end{cases} \quad (\text{A.108})$$

Then

$$\langle Y(t_2)Y(t_1) \rangle = \sigma^2 \min(t_2, t_1) \quad (\text{A.109})$$

which coincides with (A.105) for  $w_1 = 0$ . That is, the integral of a Gaussian process is a Wiener process.